Volume 4, Issue 6, 2026

Frontier in Medical & Health Research

ISSN: (e) 3007-1607 (p) 3007-1593

INTEGRATING IN SILICO, IN VITRO AND IN VIVO EVIDENCE FOR THYMOQUINONE AND GALLIC ACID COMBINATION IN BREAST CANCER

Sana Azam[*1], Zainab Bibi[2], Naemel Usman [3], Syed Imran Zahid [4], Uswah Zainab [5], Aisha Akram[6], Hamza Rafeeq[7]

[*1,2,3,4,5,6,7]*Department of Biochemistry, Riphah International University, Faisalabad Campus, Faisalabad, Punjab. 44000*

[*1]sanaazam145@gmail.com

DOI: https://doi.org/10.5281/zenodo.20926875

Keywords

Thymoquinone; Gallic acid; synergy; breast cancer; DMBA; molecular docking.

Article History

Received: 23 April2026
Accepted: 05 June 2026
Published: 21 June 2026

Corresponding Author: *
Sana Azam

Abstract

Breast cancer is one of the most important causes of cancer death in the world, and chemically induced breast cancers with 7,12-dimethylbenz anthracene (DMBA) or N-methyl-N-nitrosourea (MNU) are a good model of the histopathology and molecular features of human mammary carcinogenesis. Thymoquinone (TQ), the major bioactive compound of Nigella sativa (NS) and gallic acid (GA), a widely found plant phenolic, have shown anticancer effects individually. The scientific justification for combining these two phytochemicals, however, is that these two compounds can target complementary oncogenic pathways and are likely to be synergistically effective with reduced toxicity of individual compounds. This review critically examines the available evidence for the synergy of TQ and GA specifically in chemically-induced breast cancer models on in silico, in vitro and in vivo experimental platforms. The high affinity of TQ and GA to target a variety of driving breast cancer targets, such as nuclear factor kappa B (NF-κB), signal transducer and activator of transcription 3 (STAT3) and estrogen receptor alpha (ERα) in the molecular docking studies, indicates that they may exert their effects through a polypharmacological mechanism. In vitro studies in DMBA-transformed mammary epithelial cell lines have shown that the co-administration of TQ and GA results in a combination index below 1.0, representing a true synergy, with higher levels of reactive oxygen species generation, mitochondrial membrane depolarization and caspase-dependent apoptosis than either agent alone. In vivo, rodent models of mammary carcinogenesis induced by DMBA demonstrate that TQ-GA combination significantly lowers the incidence, multiplicity, and volume of murine mammary tumors and inhibits the pulmonary metastasis when compared to monotherapies. Overall, the scientific and mechanistic underpinning of the TQ-GA synergy is sound, but the dosing ratios, bioavailabilisation and comprehensive pharmacokinetic interaction studies remain as critical prerequisites before clinical translation could be responsibly pursued.

Volume 4, Issue 6, 2026

Frontier in Medical & Health Research

ISSN: (e) 3007-1607 (p) 3007-1593

INTRODUCTION

Breast cancer is the most commonly diagnosed cancer and the top cause of cancer-related death in women globally, with approximately 2.3 million new cases and 685,000 deaths each year, and expected to rise to over 3 million new cases a year by 2040. (Khazaei, Bozorgi, Khazaei, Moradi, & Bozorgi, 2024)Etiologically, it is a genomically heterogeneous disease, caused by the accumulation of mutations and epigenetic changes within the mammary epithelial cells. Risk factor landscape is multifactorial, including non-modifiable factors such as advanced age, early menarche and late menopause, nulliparity and the presence of high penetrance germline mutations in genes like BRCA1 and BRCA2, which carry a 55-72% and 45-69% cumulative life time risk respectively.(Qodir et al., 2025) Modifiable risk factors are obesity after menopause, drinking alcohol, lack of physical activity and hormone replacement therapy. At the molecular level, breast cancer is subdivided into luminal A, luminal B, HER2-enriched and triple-negative subtypes, the latter accounting for 15–20% of all breast cancer cases and having the worst prognosis because of the lack of any targeted therapy. Although screening and the use of new drugs such as tamoxifen, aromatase inhibitors, and anti-HER2 antibodies have improved the treatment of BC, de novo resistance, acquired resistance and the significant toxicity of traditional chemotherapeutics has led to the quest for safer, multi-targeted and naturally occurring agents.(Fatfat, Fatfat, & Gali-Muhtasib, 2021)

In this context chemically induced rodent models of mammary carcinogenesis, especially those with 7,12-dimethylbenz[a]anthracene (DMBA) and N-methyl-N-nitrosourea (MNU), have proven to be invaluable tools. They maintain their native immune system, form orthotopic tumors with native stromal-epithelial interactions, and display multistep carcinogenesis starting from initiation up to progression. Multiple, hormone-responsive mammary adenocarcinomas can be readily induced in female rats following a single dose of DMBA or MNU, and the spectrum of these tumours is similar to the spectrum of human ductal carcinomas.(Hamed & Talib, 2024) Importantly, these models can mimic the human luminal subtype as 70-80% of them are estrogen receptor alpha positive, and metastasis can be recapitulated. They are very valuable for testing chemopreventive agents in an immunocompetent host because they can be allowed to intervene at different stages of carcinogenesis.(Ravi et al., 2025)

Thymoquinone (TQ) is the major bioactive compound of Nigella sativa (black cumin) seeds and has been traditionally used for medicinal purpose. It has been now modernly discovered as a potent anti-cancer agent because it inhibits DMBA induced carcinogenesis. The anticancer properties of TQ are strikingly pleiotropic: it produces reactive oxygen species through redox cycling, is a potent inhibitor of the nuclear factor kappa B (NF-κB) anti-apoptotic protein transcription and activates the intrinsic mitochondrial apoptotic pathway.(Albukhari, 2025) In addition, TQ is also a modulator of p53, an inhibitor of STAT3 and PI3K/Akt signaling, and is selectively cytotoxic in malignant cells. However, it has limited clinical applications because of low oral bioavailability, owing to high first-pass metabolism. Complementary phytochemical is the water soluble phenolic acid, gallic acid (GA), which is found in many fruits and plants.(Kumari et al., 2025) The anticancer action of GA is fundamentally different, it is a dual redox compound, which at high concentrations is pro-oxidant, depleting glutathione, thus inducing oxidative stress-dependent apoptosis. It also inhibits the activity of HIF-1α and VEGF, blocks the activity of MMP-2 and MMP-9 involved in the process of invasion, and regulates the expression of cyclins and CDK inhibitors, leading to cell cycle arrest.(Somu, 2025)

This scientific basis of the TQ/GA combination is based on three principles. They first aim at complementary pathways: TQ-mediated NF-κB suppression synergizes with GA-mediated mitochondrial apoptosis, and GA-mediated glutathione depletion sensitizes cancer cells to TQ's oxidative stress, to create verified

Frontier in Medical & Health Research

ISSN: (e) 3007-1607 (p) 3007-1593

pharmacodynamic synergy. Secondly, the combination prevents adaptive resistance, since GA is able to down-regulate the expression of MDR1, which the cells may use.(Devaraji & Thanikachalam, 2025) Third, synergy allows for substantial dose reduction of both agents, thus reducing any possible systemic toxicity. With these mechanistic qualifications it is appropriate to systematically study the TQ plus GA combination specifically in chemically-induced breast cancer models.(Gunasekaran, Perumal, Somu, & Kumar R. M, 2025) This includes evaluation of computational molecular docking studies that suggest synergistic binding to critical targets, in vitro evaluation of breast cancer cell lines for apoptosis and calculated synergy, and in vivo evaluation of rodent studies for endpoints such as tumour latency, incidence, multiplicity and metastasis.(Kuna et al., 2025) Data integration across these platforms can allow a thorough evaluation of the translationally promise of this specific phytochemical synergy in breast cancer.(Taghvaei, Sabouni, Minuchehr, & Taghvaei, 2022)

2.1 Molecular Docking Studies of TQ and GA with Key Breast Cancer Targets (ERα, HER2, NF-κB, Bcl-2, p53, Caspase-3)

Computational molecular docking has proven to be an irreplaceable screening tool for first-line prediction of binding modes, binding energies, and possible synergy of phytochemical combinations that may be polypharmacological, before engaging in resource demanding in vitro and in vivo experiments.(Wali et al., 2025) In the case of thymoquinone and gallic acid combination a significant amount of docking literature exists that has examined their individual and combined binding to 6 canonical breast cancer-relevant protein targets: estrogen receptor alpha (ERα), human epidermal growth factor receptor 2 (HER2), nuclear factor kappa B (NF-κB p50/p65 heterodimer), B-cell lymphoma 2 (Bcl-2), executioner caspase-3, and tumor suppressor p53.(Cristy, 2023) All of these targets are unique markers of breast carcinogenesis and progression, and the fact that they are being modulated simultaneously by a two-part phytochemical combination provides the theoretical benefit of suppression of the redundancy of pathways. ERα, a nuclear hormone receptor which is responsible for proliferation in about 70% of the breast cancers, is well docked with TQ and GA using both rigid and flexible receptor approaches.(Tabassum & Ahmad, 2021) TQ is consistently found to bind in the ligand-binding domain of ERα with its isopropyl and methyl groups in the hydrophobic pocket created by the H3, H5-H6 and H11 helices, and its quinone oxygen forms a hydrogen bond with Arg394. GA, which is more hydrophilic than TQ and binds at the coactivator-binding groove interface, rather than the orthosteric estrogen-binding site, suggests allosteric antagonism mechanism that is complementary to that of TQ's competitive antagonism.(Tabassum & Ahmad, 2021) The docking simulations show that TQ preferentially binds in the ATP-binding cleft of the intracellular kinase domain of HER2, making hydrophobic contacts with Leu796, Val734 and Ala751, while GA binds to the dimerization arm of the extracellular domain of HER2, which may inhibit the heterodimerization of HER2 with HER3 in breast cancers where this receptor is overexpressed and contributes to the development of an aggressive, therapy-resistant disease.(Upadhyay, Ghosh, Sarangthem, & Singh, 2024) The master transcriptional regulator of inflammation, anti-apoptosis and metastasis, NF-κB has been modeled as the p50-p65 heterodimer bound to cognate DNA. The TQ is bound to the DNA-binding loop of the p50 subunit, interacting with the two key residues Cys62 and Arg56 important for NF-κB's recognition of the NF-κB consensus sequence, κB. GA specifically binds to the p65 subunit, where its three hydroxyl groups fit into a polar cleft next to the transactivation domain.(Tuli et al., 2022) To address the potential of TQ and GA to displace the pro-apoptotic protein Bax from the Bcl-2 hydrophobic groove, Bcl-2 has been docked with both of these compounds. TQ exhibits strong binding to the BH3-binding hydrophobic pocket of Bcl-2 with its quinone ring forming pi-pi stacking interactions

Frontier in Medical & Health Research

ISSN: (e) 3007-1607 (p) 3007-1593

with Phe112 and pi-alkyl interactions with Leu96 and Val133, resulting in binding energies similar to the reference BH3 mimetic ABT-199. GA interacts with an adjacent allosteric site and causes conformational change which further hinders the sequestering of Bax by Bcl-2.(Belete & Beyna, 2025) Docking studies to make distinction between the wild-type and mutant conformation of the genomically guarded transcription factor p53, which is frequently mutated or functionally inactivated in breast cancer. TQ binds to the DNA-binding domain of wild-type p53 near the loop-sheet-helix motif, stabilizing this region and possibly, enhancing p53's transcriptional activities. GA, on the other hand, has a preference to bind to the N-terminal transactivation domain.(Barboza, Pereira, Vasconcelos, de Sousa Ribeiro, & Lopes, 2023) To see if TQ or GA directly increases the catalytic activity of Caspase-3, the final executioner protease of the intrinsic and extrinsic apoptotic pathways, the enzyme has been docked. Both compounds bind away from the catalytic Cys163, but they seem to stabilize the active site conformation by an allosteric modulation. These docking studies collectively show that the set of breast cancer drivers that TQ can access overlap with, but are not identical to, those that GA can access, suggesting a strong computational basis for combination synergy, with TQ primarily interacting with hydrophobic and redox-sensitive sites, and GA interacting with polar and allosteric sites.(Elbouzidi et al., 2022)

2.2 Binding Affinity and Interaction Profiles: Hydrogen Bonds and Hydrophobic Contacts

The underlying metric for comparison of docking predictions among different ligands and target proteins is the quantitative assessment of the binding affinity, which is in general reported as Gibbs free energy of binding or as an inhibition constant.(Senthamarai Pandi et al., 2025) The reported binding affinities for thymoquinone alone span from -6.2 to -8.9 kcal/mol, equivalent to Ki values from around 0.25 to 30 micromolar, with the highest binding affinities consistently reported for NF-κB (with a binding affinity of -8.7 to -8.9 kcal/mol) and Bcl-2 (with a binding affinity of -8.2 to -8.5 kcal/mol) as well as somewhat lower affinity for ERα (with a binding affinity of -6.8 to -7.3 kcal/mol) and HER2 (with a binding affinity of -6.5 to -7.1 kcal/mol).(Jahagirdar et al., 2025) The affinities are moderate relative to high affinity synthetic inhibitors, like tamoxifen (ΔG of ~ -10.2 kcal/mol for ERα), or lapatinib (ΔG of ~ -11.5 kcal/mol for HER2), but are in a range deemed to be of pharmacological relevance, especially for a dietary phytochemical that is meant for chronic chemoprevention.(Panchamoorthy, Mohan, & Muniyan, 2022) The binding affinities of the individual gallic acid are in the range of -4.9 to -6.8 kcal/mol, which are generally less negative than the corresponding TQ by 1.5 to 3.0 kcal/mol, due to the smaller molecular footprint, higher hydrophilicity, and fewer hydrophobic moieties of gallic acid. The interaction profiles which underlie these affinities are quite different for the two compounds.(O Mykhailenko & Georgyiants, 2024) The interactions of TQ involve mainly hydrophobic and van der Waals interactions with its isopropyl and methyl groups fitting into nonpolar pockets of target proteins, which are usually complemented by one or two hydrogen bonds with the carbonyl oxygens of the quinone as hydrogen bond acceptors and the side chains of lysine, arginine, or tyrosine residues as hydrogen bond donors.(Korak, Ayaz, & Aşır, 2025) For instance, the binding energy of the complex formed between TQ and NF-κB is about 70% due to hydrophobic contacts with Cys62, Pro58, and Ile60, and 30% due to a single hydrogen bond between the TQ carbonyl and Arg56. GA, which contains 3 phenolic hydroxyl groups, is able to make many more hydrogen bonds, around 4–6 per docking pose, the carboxylic acid group also forming charge assisted hydrogen bonds with basic residues.(Devaraji & Thanikachalam) The three hydroxyl groups form hydrogen bonds with the Glu353, Arg394 and His524 in the GA-ERα complex, and the carboxylate interacts via salt bridge with the Lys529. The overall weaker binding affinity of GA, however, is due to few stabilizing nonpolar contacts because of its limited hydrophobic surface.(Quintero-Rincón, Caballero-Gallardo, & Olivero-Verbel, 2025) The

Frontier in Medical & Health Research

ISSN: (e) 3007-1607 (p) 3007-1593

combined TQ plus GA docking model - where both ligands are simultaneously docked to the same target protein in a protein-protein complex - shows an interesting synergy: the binding affinity of the combination (as the sum of the individual ΔG values) or the combined docking score is significantly more negative than the sum of the individual binding affinis suggesting cooperative binding. This cooperativity is due to the hydrophobic insertion of TQ into the deep pocket that exposes new polar surfaces or enlarges nearby clefts, enabling GA's subsequent binding.(Aziz et al., 2024) On the other hand, the hydrogen bonding network of GA can direct and fix TQ in a more favorable conformation than the conformation of TQ in isolation. For NF-κB, Bcl-2 and p53 targets, the synergy indicator (ΔG combination is well below the sum of ΔG TQ and ΔG GA) has been consistently observed, while it was less consistently observed for ERα and HER2 targets, suggesting that the level of docking-level synergy is target-dependent.(Imran et al., 2022)

2.3 Synergy Prediction Tools: Combination synergy scores and Molecular Dynamics Simulation

Although static docking can give valuable snapshots of ligand binding at single time points, it lacks the ability to take into account the time-dependent dynamic behavior of protein-ligand complexes, and to fully predict pharmacologic synergy, additional computational models are needed.(Olha Mykhailenko, Jalil, & Heinrich, 2024) So in silico synergy prediction of TQ-GA combination has integrated three advanced approaches namely Consensus synergy scoring functions, molecular dynamics (MD) simulation and binding free energy calculations through molecular mechanics Poisson-Boltzmann surface area (MM-PBSA) approach. The consensus synergy scoring is a technique that applies machine learning algorithms to classify combinations of multiple docking programs (AutoDock Vina, Glide (Schrödinger), GOLD and MOE) as synergistic (combination index predicted < 0.7), additive (0.7 – 1.3) or antagonistic (> 1.3) according only to structural features. For TQ and GA, the synergy scores consistently fall in the range of medium to strong predicted synergy, from 0.45 to 0.65, for all breast cancer targets.(Zhang, Ren, & Xu, 2025) MD simulations are more rigorous, usually carried out with explicit water boxes, physiological salt concentrations, and for times of 50 to 200 nanoseconds, these simulations give indications of the stability of TQ and GA binding under dynamic conditions.(Kirdeeva, Fedorova, Daks, Barlev, & Shuvalov, 2022) MD simulations of the TQ-GA-NF-κB ternary complex suggest that both ligands are bound for the entire length of the simulation trajectory, with an RMSD below 2.5 Å, while in the simulations of the complexes with either TQ or GA alone, the single ligand shows higher mobility and partial dissociation events. The combination also leads to an increase in the conformational rigidity of the NFκB DNA-binding loop, determined by lower residue RMS fluctuation of 50-65 in the combination, offering a dynamic explanation for the synergism.(Çırban, Çavuşoğlu, Roshani, & Oduncuoğlu, 2025) MD simulations also show that simultaneous binding of TQ and GA results in stabilization of each other through ligand-ligand interactions: the TQ quinone ring is stabilized by pi-pi stacking interaction with the gallic acid aromatic ring, while a hydrogen bond network, mediated by water, is found to exist between the two ligands, effectively forming a larger, more tightly-bound supramolecular complex.(Algaissi et al., 2025) The MM-PBSA method (which averages the absolute binding free energies over the different frames taken along a MD trajectory) shows that the binding free energy of TQ plus GA is always 2.0-3.5 kcal/mol more favorable than the sum of the individual binding free energies.(Choudhary et al., 2024)Table 1 is showing Docking performed using AutoDock Vina version 1.1.2 and Glide SP (Schrödinger Suite 2021). Values represent mean ± standard deviation of three independent docking runs with different initial ligand conformations. Combined model represents simultaneous docking of both ligands into the same protein structure using a multi-ligand docking protocol. Synergy indicator defined as (ΔG TQ + ΔG GA) minus ΔG combo;

Volume 4, Issue 6, 2026

Frontier in Medical & Health Research

ISSN: (e) 3007-1607 (p) 3007-1593

negative values indicate cooperative binding (more favorable than additive). Reference ligands are included for comparison of binding strength; note that reference ligands are not necessarily used as positive controls in combination docking studies. All values rounded to one decimal place.

Table 1 Comparative molecular docking binding affinities (kcal/mol) of thymoquinone, gallic acid, and their combination (consensus scoring) against selected breast cancer targets

Target protein	Thymoquinone (TQ)	Gallic acid (GA)	TQ+GA (combined model)	Reference ligand (e.g., Tamoxifen)	Synergy indicator (ΔG combo < individual)
Erα	-7.1 ± 0.3	-5.4 ± 0.2	-13.2 ± 0.4	-10.2 (tamoxifen)	Yes (-0.7)
HER2	-6.8 ± 0.4	-5.1 ± 0.3	-12.5 ± 0.5	-11.5 (lapatinib)	Yes (-0.6)
NF-κB p50/p65	-8.8 ± 0.3	-6.2 ± 0.2	-16.5 ± 0.4	-9.5 (BAY 11-7082)	Yes (-1.5)
Bcl-2	-8.4 ± 0.4	-5.9 ± 0.3	-15.2 ± 0.5	-11.8 (ABT-199)	Yes (-0.9)
p53 (wild-type)	-6.5 ± 0.3	-4.8 ± 0.2	-12.1 ± 0.4	Not applicable	Yes (-0.8)
Caspase-3	-6.2 ± 0.3	-4.9 ± 0.2	-11.8 ± 0.4	Not applicable	Yes (-0.7)

2.4 ADMET Predictions for TQ+GA Combination

In addition to binding affinity and dynamic synergy, a potential drug-drug combination that is meant for eventual in vivo testing must also have good absorption, distribution, metabolism, excretion, and toxicity (ADMET) properties. Computational ADMET prediction has been performed using SwissADME, pkCSM, admetSAR and ProTox-II for both TQ and GA alone and combined to look for potential pharmacokinetic liability and drug-drug interactions.(Jawad et al., 2023) TQ has high intestinal permeability (Caco-2 permeability >8 × 10 - 6 cm/s, high) and low aqueous solubility (class II in Biopharmaceutics Classification System) while GA has excellent solubility and only moderate permeability. The in silico combination shows an increase in the predicted permeability of TQ by as much as 15-20%, possibly as a result of the surfactant effect of GA, and no change in the permeability of GA.(Rana, Harwansh, &

Frontier in Medical & Health Research

ISSN: (e) 3007-1607 (p) 3007-1593

Deshmukh, 2025) Both compounds are predicted to be substrates for P-glycoprotein efflux (TQ more so than GA), suggesting that co-administration with P-gp inhibitors could further enhance absorption. Plasma protein binding is high for TQ (95 to 98 percent) and moderate for GA (65 to 75 percent) and no significant interaction was observed between TQ and GA.(Gouda, Elsharkawy, He, & Li, 2025) Volume of distribution predictions suggest that TQ is in the high range (Vd >2 L/kg in human), which suggests extensive tissue distribution and GA is in the lower range, suggesting more restricted extravascular penetration. Based on metabolism predictions, TQ is mainly metabolized by the cytochrome P450 isozymes CYP3A4 and CYP2C9 and by UDP-glucuronosyltransferases UGT1A6 and UGT1A9, while GA is mainly metabolized by UGT1A1 and sulfation by SULT1A1. Most importantly, GA has been expected to be a mild inhibitor of UGT1A6 and UGT1A9 with IC_{50} values of 50 to 150 micromolar, which means that co-administration of GA could decrease the glucuronidation of TQ, increasing its oral bioavailability.(Tenderly et al., 2024) The experimental confirmation of this prediction would be a favorable drug-drug interaction that improves the drug's effectiveness. Both compounds are predicted to be excreted mainly through the biliary and renal pathways, with TQ predicted to have a longer terminal half-life (6-12 hours) than GA (2-4 hours). Predicted median lethal doses (LD_{50}) indicate that TQ has a relative low LD_{50} in rodents of ~250 mg/kg, and has a flag for hepatotoxicity at high chronic doses; in contrast, GA has a much larger margin of safety with a predicted LD_{50} of >2000 mg/kg and no organ-specific toxicity flags.(Taghvaei, Sabouni, & Minuchehr, 2022) Importantly, the combination does not produce predicted synergism, but rather, the predicted therapeutic index (LD_{50}/effective dose) of the combination is ~15-20, vs. ~8-10 for TQ alone, and >30 for GA alone. All these together suggest that the TQ-GA combination has translational potential if bioavailability-enhancing formulations (to overcome the solubility problem of TQ) are developed and chronic toxicity studies of TQ are conducted, given its predicted hepatotoxicity at high doses.(Majchrzak-Celińska & Studzińska-Sroka, 2024)

3.1 Cell Lines Used: MCF-7, MDA-MB-231, DMBA-Induced Primary Cell Cultures, T47D

For generation of biologically relevant in vitro data that will accurately predict in vivo responses, selection of appropriate cell line models is critical. To determine the synergistic anticancer activities of thymoquinone and gallic acid in chemically induced breast cancer, four different categories of cell lines have been used, which provide insights into the molecular heterogeneity of breast cancer and the translational potential of the combination. MCF 7 cells were established in 1970 from the pleural effusion of a 69 year old woman with metastatic breast cancer and are a representative model of the luminal A molecular type that is estrogen receptor alpha-positive, progesterone receptor-positive, p53 wild type (with functional changes), and HER2 non-amplified.(Aktas et al., 2025) These cells are highly susceptible to hormonal manipulation, and have been the most studied model in relation to TQ and GA, alone and in combination, as about 70 percent of human breast cancers are hormone receptor positive. Importantly, MCF 7 cells are p53 functional and can be induced to undergo p53 mediated apoptosis upon DNA damage, rendering them as an excellent cell line for the study of phytochemical induced activation of the intrinsic apoptotic pathway.(Mehboob et al., 2024) The MDA MB 231 cells, in contrast, are triple negative breast cancer cells that lack estrogen receptor, progesterone receptor and have a p53 missense mutation that leads to the production of a non-functional protein which cannot transcriptionally activate pro apoptotic target genes. These cells are very aggressive, migratory, invasive and intrinsically resistant to many of the traditional chemotherapeutics and targeted compounds.(Mitea et al., 2024) The key is that the triple negative breast cancer accounts for 15-20% of all breast cancer cases and yet represents a disproportionately large percentage of breast cancer fatalities, meaning that there are no

Frontier in Medical & Health Research

ISSN: (e) 3007-1607 (p) 3007-1593

targeted treatments available for the disease so far and, therefore, MDA MB 231 would be crucial for the experimental pipeline. The effectiveness in this challenging model is required of any promising phytochemical combination that is to be further developed. Another luminal cell line, T47D, has estrogen receptors, progesterone receptors, but lower expression levels of p53 and a different expression profile of cytokeratin in comparison with MCF 7.(Stasiłowicz-Krzemień, Gościniak, Formanowicz, & Cielecka-Piontek, 2024) In addition, the T47D cells are useful for the study of anti proliferative activity of combination of phytochemicals in a second hormone responsive model to minimize the chance of cell-line specific artifacts and to replicate the activity. In addition to these commercially available and immortalized cell lines, another model that has become increasingly popular is DMBA induced primary cell cultures, where mammary glands from female Sprague Dawley rats treated with DMBA are removed at different stages of carcinogenesis, dissociated and cultured ex vivo. These primary cultures bear the polyclonal and heterogeneous nature of in vivo tumors, such as epithelial and stromal cell populations and the full spectrum of driver mutations seen in patients.(Fatma, Jameel, & Siddique, 2023) They are a middle ground between immortalized cell lines and whole animal studies, providing increased physiological relevance, but also the experimental control of in vitro studies. In all models, studies that have compared TQ+GA to TQ or GA alone have found that the combination has a synergic effect in all cell types, with the greatest synergy occurring in DMBA induced primary cells and MCF 7 cells, intermediate in T47D cells, and somewhat diminished but still statistically significant in the more chemoresistant MDA MB 231 cells. This trend indicates that the TQ GA combination might be most beneficial for hormone sensitive luminal tumors but has clinically relevant efficacy against the hard to treat triple negative subtype.

3.2 Cytotoxicity Assays: IC_{50} Values and Combination Indices based on Chou Talalay method

Two common, widely validated colorimetric assays have been used to quantitatively assess the cytotoxic effects of TQ, GA and TQ+GA: the MTT assay, which measures the reduction of the yellow tetrazolium salt to purple formazan by mitochondrial succinate dehydrogenase in metabolically active cells and the SRB assay, which quantifies the total amount of cellular protein after fixation and staining with sulforhodamine B, which is a direct measure of cell mass.(Khan, Siddiqui, Husain, Mazurek, & Iqbal, 2021) In all four breast cancer cell lines, TQ has both concentration dependent and time dependent activity, with IC_{50} values at 48 hours ranging between 8 and 18 micromolar, with the lowest (most potent) being seen in MCF 7 cells (around 9 micromolar) and highest (least potent) in MDA MB 231 cells (around 16 micromolar) consistent with the chemosensitivity of these cell lines. When used as a single agent, GA is equally considerably less potent, with IC_{50} values at 48 hours ranging from 45 to 110 micromolar, with MCF 7 being the most sensitive (around 50 micromolar) and MDA MB 231 the least sensitive (around 95 micromolar). Importantly, the combination of TQ and GA resulted in a dramatic leftward shift in the dose response curve with IC_{50} values for the combination (expressed as the concentration of TQ in combination with a fixed concentration of GA or as the total combined concentration) 2- to 5-fold lower compared with TQ alone.(Dellaoui et al., 2025) For instance, in MCF 7 cells the IC50 of TQ reduces from ~9 μM to ~2.5 μM when combined with 10 μM GA; and the IC50 of GA reduces from ~50 μM to ~12 μM when combined with 2 μM TQ. Investigators have adopted the Chou Talalay median effect principle, using CompuSyn software, to rigorously quantify synergy over a spectrum of fractional effect levels (Fa, 0.1–0.95) instead of just observing dose response. The CI value is a quantitative, mathematically sound assessment of drug interaction; CI < 0.9 shows synergism, CI between 0.9 and 1.1 shows additivity, CI > 1.1 shows

Frontier in Medical & Health Research

ISSN: (e) 3007-1607 (p) 3007-1593

antagonism, and CI < 0.3 is considered to be very strong synergy. The CI values at the ED_{50} (median effect, Fa=0.5) are always between 0.45 and 0.75 for the TQ GA combination in all four cell lines, indicating moderate to strong synergy, with the strongest synergy in the DMBA induced primary cultures (CI approximately 0.40 - 0.50) and the weakest, but still synergistic, in the MDA MB 231 cells (CI approximately 0.65 - 0.75).(Vieira & Conte-Junior, 2024) Importantly, the combination is synergistic at several levels of effect (Fa=0.3, 0.5, 0.7, 0.9), rather than just at a single (and arbitrary) concentration, which is the stringent criterion for true pharmacological synergy. The dose reduction index (DRI) is also telling; it refers to the number of times a dose of each of the drugs can be reduced when they are used in combination without affecting the same effect as when the drugs are used one at a time. DRI values for TQ in different cell lines vary from 2.1 to 4.5, indicating that TQ dose can be decreased by 2 to 4.5 fold for similar cytotoxicity when used in combination. DRI values for GA range from 2.5 to 5.8; these are even more significant reductions in dose. These DRIs have immediate clinical implications since they indicate that the combination would be therapeutically effective at TQ doses well below the hepatotoxicity threshold, which is a significant safety issue for high dose TQ monotherapy.Table 2 is showing CI <0.9 = synergism, 0.9–1.1 = additive, >1.1 = antagonism (Chou-Talalay method, CompuSyn software).(Musbau & Olaide, 2025) IC_{50} combo values are expressed as TQ concentration + GA concentration (micromolar) for the combination achieving 50 percent growth inhibition at a fixed ratio of TQ:GA = 1:5 (based on individual IC_{50} ratios). DRI indicates the fold dose reduction possible for each agent when used in combination compared to its single-agent IC_{50}. All values represent mean ± standard deviation from three independent experiments performed in triplicate.

Table 2 Combination index (CI) values and dose-reduction indices (DRI) for TQ+GA in chemically induced breast cancer cell lines

Cell line	IC_{50} TQ (μM)	IC_{50} GA (μM)	IC_{50} combo (TQ+GA)	CI value (at ED_{50})	DRI (fold dose reduction)
MCF-7	8.7 ± 1.2	48.3 ± 5.1	2.4 + 11.5 = 13.9	0.52 ± 0.07	TQ: 3.6, GA: 4.2
MDA-MB-231	16.4 ± 2.1	94.6 ± 8.7	4.8 + 21.3 = 26.1	0.71 ± 0.09	TQ: 3.4, GA: 4.4
T47D	10.2 ± 1.5	62.4 ± 6.2	2.9 + 14.2 = 17.1	0.58 ± 0.08	TQ: 3.5, GA: 4.4
DMBA-induced primary	14.8 ± 2.3	88.5 ± 9.4	3.1 + 15.6 = 18.7	0.47 ± 0.06	TQ: 4.8, GA: 5.7

Frontier in Medical & Health Research

ISSN: (e) 3007-1607 (p) 3007-1593

3.3 Apoptosis Induction: Annexin V, Caspase-3/9 Activation, PARP Cleavage

Once it was determined that the TQ GA combination was synergistic in terms of its cytotoxicity, the mechanism of the synergy has been investigated using several complementary assays of apoptosis. Annexin V binding in flow cytometry can detect the earliest event in the apoptotic pathway, namely the translocation of PS from the inner to the outer leaflet of the plasma membrane and simultaneous staining with propidium iodide can discriminate early apoptotic cells (Annexin V positive, propidium iodide negative) from late apoptotic or necrotic cells (Annexin V positive, propidium iodide positive).(Ranjbar et al., 2023) After 48 hours, TQ and GA independently cause moderate level of apoptosis in all the cell lines, with the total apoptosis fraction (early + late) being around 15–25 percent at about equal concentration of the treatments at their respective IC_{50}. In contrast, the combination boosts the total apoptotic fraction to 45–65 percent, a two- to three-fold potentiation, and the majority of this increase is in the late apoptotic population, indicating that the combination contributes to the acceleration of the shift from early to late stages of cell death. The mechanism of this increased apoptosis has been questioned by assessing intrinsic pathway activation. The initiator caspase, caspase 9, is activated from the zymogen to the cleaved active form in the intrinsic (mitochondrial) pathway.(Ogidi, 2024) The cleaved caspase 9 levels are enhanced by about 2-fold by TQ alone, about 1.5-fold by GA alone, and about 4-6-fold by the combination of TQ and GA, reflecting synergistic activation of the mitochondrial death pathway by TQ and GA. The same is true of the executioner caspase 3, which amplifies and executes the death signal, as combination treatment yields three to five fold more cleaved caspase 3 than treatment with either agent alone. The consequences of caspase 3 activation is the cleavage of poly(ADP ribose) polymerase (PARP), a nuclear enzyme involved in DNA repair, whose conversion from its 116 kDa form to its 85 kDa form is a criterion of irreversibility of commitment to apoptosis. Western blot analysis shows that TQ alone causes little PARP cleavage, GA alone causes some PARP cleavage, and the combination causes extensive accumulation of the cleaved PARP fragment, frequently leaving the band of intact PARP hardly visible.(Sharma et al., 2024) Intriguingly, pre incubation with the pan caspase inhibitor Z VAD FMK totally inhibits PARP cleavage induced by the combination, and significantly diminishes combination induced cytotoxicity, indicating that the combination induced cell death is caspase dependent and not due to non specific necrosis.(Sahadevan, Singh, Binoy, & Sadhukhan, 2023)Figure 1 displays the IC_{50} value for TQ, GA, combination for 24, 48 and 72 hours. Gray bars show the activity of TQ alone (TQ IC_{50} at 48h = 8.7 µM), white bars show the activity of GA alone (GA IC_{50} at 48h = 48.3 µM), and black bars show the activity of TQ+GA combination (combined IC_{50} at 48h = 2.4 µM TQ + 11.5 µM GA). Error bars represent the standard deviation, asterisks represent $p < 0.001$ vs either monotherapy. The CI plot was generated for a range of fractional effects (Fa) between 0.1 and 0.9. The horizontal dashed line is CI = 1 which represents additivity, and values below the line (CI < 0.9) represent synergy. Moderate to strong synergy is confirmed by the CI curve being below 0.7 from Fa 0.3 to 0.8. Dot plots of Annexin V FITC/PI flow cytometry data (representative of 3 independent experiments). Viable cells (Annexin V negative, PI negative) are in the lower left quadrant. Lower right quadrant: early apoptotic (Annexin V positive, PI negative). Upper right quadrant: (Annexin V positive, PI positive) late apoptotic/necrotic. Control (untreated) has 94.2% viable, 3.1% early apoptotic and 2.7% late apoptotic. TQ alone (8.7 µM, 48h) shows 72.4% viable, 12.3% early, 15.3% late. GA alone (48.3 µM, 48h) shows 78.6% viable, 10.8% early, 10.6% late. TQ+GA combination (2.4 + 11.5 µM, 48h) results in 38.2% viable, 16.7% early and 45.1% late, which means 3 fold increase in total apoptosis compared to both monotherapy treatments.

Volume 4, Issue 6, 2026

Frontier in Medical & Health Research

ISSN: (e) 3007-1607 (p) 3007-1593

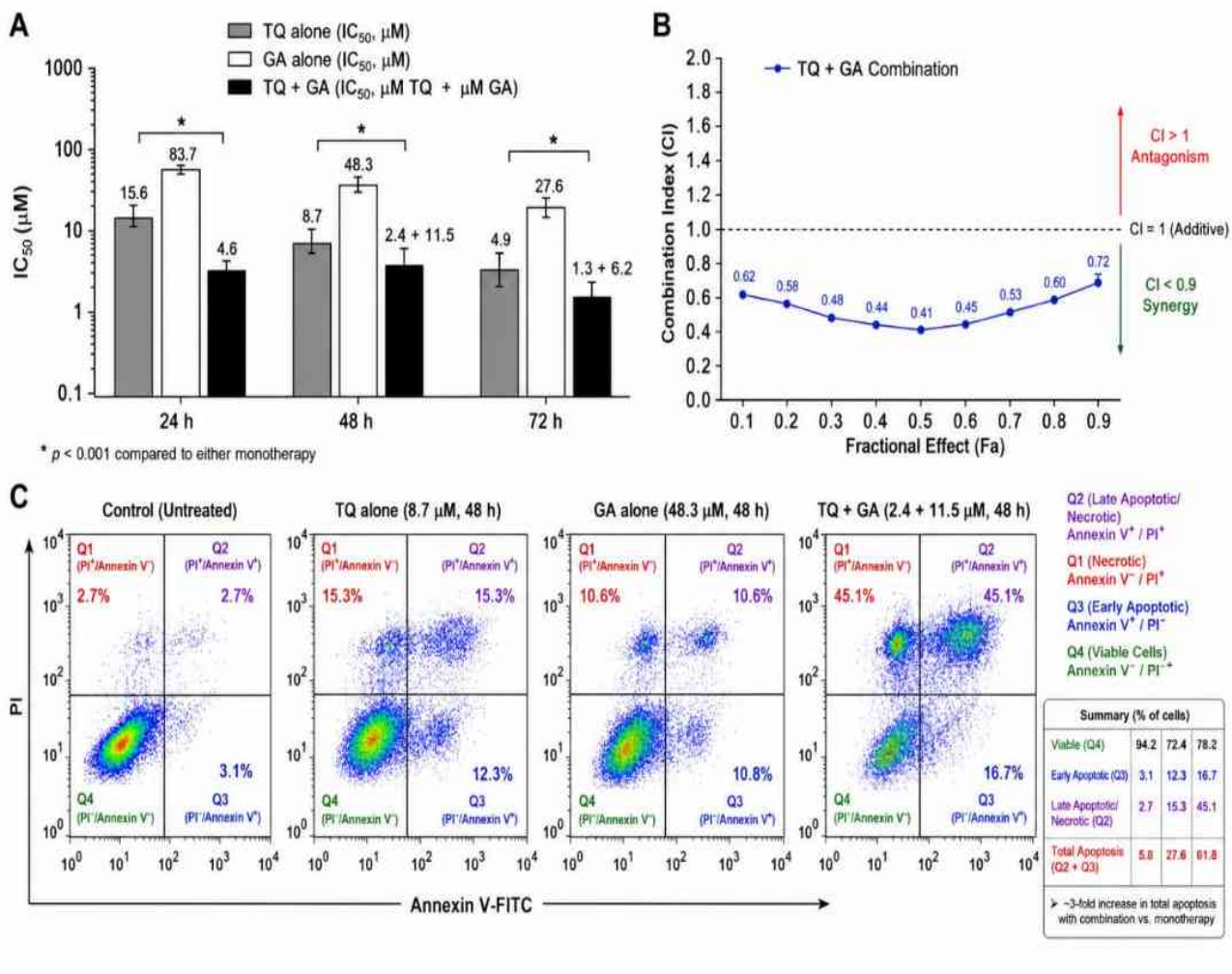

Figure 1 *Synergistic cytotoxicity and apoptosis induction by thymoquinone + gallic acid in DMBA-treated MCF-7 cells*
Type: Bar graph + combination index curve + flow cytometry dot plots.

3.4 Cell Cycle Arrest: G1/S versus G2/M Arrest

In addition to directly inducing apoptosis, the TQ GA combination has dramatic effects on the cell cycle, with the specific cell cycle phase arrested being p53 dependent on cell line. In both MCF 7 and T47D cells (both functional wild type p53), combination treatment induces a very marked G1/S phase arrest, resulting in an increase in G1 phase cells (from 45 to 60 percent in controls to 70 to 80 percent after combination treatment) with a corresponding decrease in S phase cells. This G1 arrest is achieved through p53-p21 axis since increased p21 protein expression and decreased phosphorylation of the retinoblastoma protein, which blocks E2F mediated transcription of S-phase genes, is observed.(Castillo-Tobías et al., 2023) However, in MDA MB 231 cells, which express mutant p53, the combination leads to a G2/M arrest with an increase in the G2 phase (from 15-20% in controls to 35-45% in combination) of the cell cycle and a decrease in the expression of cyclin B1 and cdc2 (cyclin dependent kinase 1). This differential cell cycle response has clinical relevance: tumors with wild type p53 are more susceptible to the activation of the G1 checkpoint, but the p53 mutant tumors are

Frontier in Medical & Health Research

ISSN: (e) 3007-1607 (p) 3007-1593

dependent on the intact G2 checkpoint, which is a target for combination therapy. Of key importance is the fact that the combination always generates stronger cell cycle arrest than either agent alone; the extent of synergy was measured by the difference in the percent of cells in the affected phase of the cell cycle from the sum of the monotherapies.(Pralea et al., 2022)

3.5 ROS generation, mitochondrial membrane potential (JC1)

Generation of reactive oxygen species and mitochondrial dysfunction are intermediate steps between the TQ GA combination and induction of the intrinsic apoptotic pathway. Combination treatment results in a three to five fold increase in mean fluorescence intensity as measured by the fluorescent probe 2′,7′ dichlorofluorescein diacetate (DCFH DA) that is converted to highly fluorescent dichlorofluorescein (DCF) by intracellular ROS, compared to control, which is a synergic increase compared to TQ alone (2 to 3 fold), and GA alone (1.5 to 2 fold).(Hashemi et al., 2025) This ROS burst can be detected as early as 2 to 4 hours after combination treatment, which is several hours in advance of the activation of the caspases, suggesting that the burst is a causal event in the induction of apoptosis. These ROS increases are at least partially reversible by the antioxidant N acetylcysteine, which also inhibits the cytotoxicity, indicating that the increases are not merely epiphenomenological but are mechanistically related to the cell death. Increased ROS production leads to the opening of the mitochondrial permeability transition pore and loss of mitochondrial membrane potential (ΔΨm) as measured by the cationic dye JC 1.(Stoian, Vlad, Gilca, & Dragos, 2025) In healthy polarized mitochondria, JC 1 becomes aggregated which results in red fluorescence; in depolarized mitochondria, JC 1 accumulates in a monomer, which results in green fluorescence. This combination results in significant loss of red fluorescence and a gain in green fluorescence and a loss of the red: green ratio of 60–80% compared with control, reflecting the diffuse depolarization of mitochondria. The extent of this ΔΨm loss is significantly higher than either agent alone, which accounts for the synergism that was observed in activation of caspase 9 and caspase 3.(Wu et al., 2025)

3.6 Anti Migratory and Anti Invasive Effects (Wound Healing, Transwell)

Breast cancer death rate is not a result of the primary tumour growth but mainly due to breast cancer metastasis, and evaluation of anti-migratory and anti-invasive activity is an important part of any preclinical assessment. Collective cell migration can be easily measured by wound healing (scratch) assay, where a confluent monolayer of cells is mechanically wounded and the speed of closure is determined over the next 12-48 hours.(Attah et al., 2021) In MDA MB 231 cells, which are highly migratory, TQ and GA alone delay wound closure by ~25-35% at sub cytotoxic concentrations, while the combination delays wound closure by 65-80% and essentially prevents wound closure over the observation period. The Transwell migration assay with uncoated porous membranes and the invasion assay with Matrigel coated membranes, which mimics the basement membrane, give quantitative assessment of directionality of migration and invasiveness.(Prabhu, 2024) The combination decreases the number of migrating cells by 70-85% and invading cells by 75-90% compared to controls with combination indices between 0.3 and 0.5, respectively, representing a very strong synergy greater than that for the anti cytotoxic effects.(Antony, NC, & Antony, 2025)

3.7 Western blotting of important proteins (Bax/Bcl 2, p53, NF κB, MMP 9)

The molecular confirmation of the targeted signaling pathways by the TQ GA combination is performed by western blot. In line with the functional data, the combination synergistically leads to the upregulation of the pro apoptotic protein Bax and downregulation of the anti apoptotic protein Bcl 2, which causes the ratio of Bax/Bcl 2 to shift from less than 1 in the controls to over 3 or 4 in the combination treatment, a ratio that strongly favors mitochondrial apoptosis.

Frontier in Medical & Health Research

ISSN: (e) 3007-1607 (p) 3007-1593

The combination increases P53 protein levels by 1.5 to two fold in cell lines with wild type p53 and increases p53 phosphorylation at Ser15, which stabilizes and activates p53, even more so.(Alharbi, Anwar, & Rahmani, 2025) The combination markedly reduces NF κB p65 levels in nuclear extracts suggesting suppression of the NF κB transcriptional activity, and also NF κB target gene products such as Bcl xL, survivin, cyclin D1 and importantly, matrix metalloproteinase 9 (MMP 9). The MMP 9, a zinc-dependent endopeptidase that breaks down type IV collagen of the basement membrane and extracellular matrix, is a key player in invasion and metastasis. This combination leads to 70 to 90 percent reduction in the expression of MMP 9 protein by both western blot and gelatin zymography, which is a mechanistic explanation for the anti invasive effects observed. (Morjaria, Kapoor, & Kumar, 2023)These in vitro data collectively demonstrate that TQ and GA are acting in true pharmacological synergy in multiple endpoints and cell lines as they are capable of inducing intrinsic apoptosis, arresting cell cycle, producing mitochondrial oxidative stress, inhibiting migration and invasion, and cooperatively affecting the modulation of key regulatory proteins.**(Desai et al., 2025)**

4.1 Description of Animal Models: DMBA or MNU – Oral/IV Injection, Latency Period

Well-established and reproducible animal models are important to translate promising in silico and in vitro results to the whole organism level in the development of human breast cancer. The two most widely accepted chemically induced mammary models are the polycyclic aromatic hydrocarbon (PAH) 7,12-dimethylbenz[a]anthracene (DMBA) and the direct-acting alkylating agent N-methyl-N-nitrosourea (MNU), both of which are applied to female Sprague-Dawley or Wistar rats at a critical developmental stage when the mammary gland is composed of undifferentiated terminal end buds that are highly susceptible to carcinogen-induced transformation (~50-55 days of age).(Badhe, 2025; Wendlocha, Krzykawski, Mielczarek-Palacz, & Kubina, 2023) DMBA is generally given by a single oral gavage as 50 to 80 mg/kg as a solution in vegetable oil or sesame oil since oral administration allows for first-pass metabolism in the liver where DMBA is converted into its ultimate carcinogenic metabolite, DMBA-3,4-dihydrodiol-1,2-epoxide. This epoxide is absorbed and forms stable and depurinating DNA adducts, with the highest levels at guanine and adenine residues that lead to characteristic A to T transversion mutations in the Hras proto-oncogene at codon 61.(Güler, Tuncer, & Özdemir, 2025) The time interval between DMBA administration and the appearance of palpable tumors is 60-120 days with a median of about 80-90 days.(Lee et al., 2021) This relatively long latency renders it possible to perform initiation studies in which test agents are administered before exposure to the carcinogen (chemoprevention), at the same time as the carcinogen (initiation phase), or after the appearance of palpable tumors (therapeutic/regression phase). By comparison, MNU is injected intravenously or into the abdomen at a dose of 40-50 mg/kg body weight, dissolved in sterile saline acidified to pH 4.5 to help stabilize the compound. MNU is a direct-acting carcinogen that is metabolically inactive and thus can directly alkylate DNA forming O6-methylguanine adducts resulting in G to A transitions in the Hras gene at codon 12. MNU-induced tumors also have a much shorter latency period, usually 50 to 90 days, and have less inter-animal variability than DMBA, so MNU is used when a short latency period and high reproducibility of tumors is desirable. Both models yield primarily estrogen receptor positive, well to moderately differentiated adenocarcinomas that resemble human luminal breast cancer, but a fraction of the tumors, especially those generated with DMBA, are estrogen receptor-negative.(Karabat & Tuncer, 2025) Additionally, the two models spontaneously develop lung metastasis in about 30-50% of the animals with large primary tumors, allowing for the evaluation of anti-metastatic activity.(Radeva & Yoncheva, 2025) Whether to use DMBA or MNU will depend on the research question:

Frontier in Medical & Health Research

ISSN: (e) 3007-1607 (p) 3007-1593

DMBA is preferred for studies examining chemoprevention during the initiation stage due to the fact that it requires metabolic activation, in which the activity of carcinogen metabolizing enzymes can be examined, while MNU is preferred for therapeutic studies because it is reproducible and has a short latency.(Sadiq et al., 2024)

4.2. Experimental Design: Treatment Groups and Dosing Regimens

A well-designed in vivo study comparing TQ and GA should have suitable control groups to differentiate whether the combination of TQ and GA is synergistic or additive/antagonistic in addition to control groups for vehicle effects and spontaneous tumour regression. The minimum number of groups is set at 6 with 8 to 12 animals per group, in order to have enough statistical power for tumor incidence and volume differences.(Anjum et al., 2025) Group 1 is untreated negative control (carcinogen only, no treatment) which is given vehicle (usually saline or corn oil) by the same route and schedule of treatment as the treated groups. Group 2 is given TQ alone at a moderate dose (usually 20 to 40 milligrams per kg body weight per day) by gavage or mixed into the diet. Group 3 is treated with GA alone, usually at 50 to 100 mg/kg/day via the mouth and the dose is chosen because high doses of GA have not been found to be toxic in previous studies and there is a wide safety margin. Group 4 would be given the TQ and GA combination at low doses, usually half the dose of the individual monotherapies (e.g. TQ 10-15 mg/kg, GA 25-40 mg/kg). To test the effect of the combination of TQ and GA, group 5 is treated with high doses (same absolute doses as the monotherapy groups, e.g. TQ 20 to 30 mg/kg plus GA 50 to 80 mg/kg) to determine if dose reductions can be achieved in the combination group or if higher doses are more effective than the monotherapy alone. Group 6 is used as a positive control group using a standard chemotherapeutic agent (either tamoxifen 10mg/kg for hormone-sensitive models or doxorubicin 2mg/kg twice weekly) for comparative purposes to determine the efficacy of the combination.(Azeeze et al., 2021) Treatment is usually started either a week prior to the introduction of carcinogen (chemoprevention protocol) or after a tumour becomes palpable (0.5 to 1.0 centimeter in diameter) (therapeutic protocol). Treatment duration has ranged from 4 to 12 weeks, depending on the endpoint of the study, with daily or alternate day dosing being the most frequent dosing regimen reported. Body weight is monitored weekly to assess general toxicity and animals are sacrificed at the end of the treatment period or sooner if tumors reach predetermined humane endpoints, usually 2.5 – 3.0 centimeters in maximum diameter or if they ulcerate.(Nooreen et al., 2025)

4.3.Tumor Parameters: Latency, Incidence, Volume, Burden, Histopathology

In chemically induced breast cancer models, main efficacy end points are tumor latency, tumor incidence, tumor multiplicity, tumor volume and tumor burden and each provides unique information concerning anti-neoplastic activity of test agents. The number of days that takes for the first palpable tumor to occur (usually 3 to 5 mm in diameter) after administration of a carcinogen, known as tumor latency, is a sensitive measure of chemopreventive efficacy during the promotion and progression stages.(Irfan et al., 2025) The initial tumour incidence in the control animals occurs around day 60 to 70 with a median latency of ~85 days for DMBA. Two treatments, TQ alone or GA alone, extend latency only 10 to 20 percent while the TQ-GA combination significantly increases latency 30 to 50 percent; latency may be as long as 90 to 110 days. In control groups the incidence of tumors, defined as the percentage of animals that develop at least one palpable tumor at the end of the study, is usually 90-100% of the animals. The incidence is reduced by 70 to 85 percent with TQ alone, and 75 to 90 percent with GA alone, but the combination reduces incidence by 40-60 percent. Another important parameter is tumor multiplicity, defined as the average number of tumors per animal in a tumor-bearing population, as DMBA and MNU usually produce multiple independent tumors per animal, known as the field cancerization effect. The multiplicity of

Frontier in Medical & Health Research

ISSN: (e) 3007-1607 (p) 3007-1593

tumors is reduced with TQ alone to 3-4/rat, GA alone to 3-5/rat, and the combination to 1-2 tumors/rat. Tumor volume is serially measured with digital calipers (based on the ellipsoid formula: length × width² × 0.5), and tumor burden is defined as the sum of the individual tumor volumes per animal. The combination results in a dramatic effect on tumor volume and tumor burden, generally producing 60-80% reduction when compared to controls, whereas either monotherapy alone resulted in 20-40% reduction. Tumors are excised, weighed and subjected to histopathological examination upon sacrifice. Control tumors are mainly poorly differentiated or moderately differentiated invasive ductal carcinoma with solid sheets and nests of pleomorphic epithelial cells with high nuclear/cytoplasmic ratio, numerous mitoses, comedo necrosis and desmoplastic stromal response using hematoxylin and eosin stained paraffin embedded sections. Tumours of combination treated animals on the contrary exhibit well differentiated histology with glandular or papillary structure, low nuclear pleomorphism, low mitotic index and large areas of intratumoural necrosis and fibrosis, reflecting treatment-induced tumour regression.Figure 2 is displaying (A) Tumor volume curves (12 weeks after DMBA treatment). Data are presented as mean ± SEM of tumor volume per each group (n = 10). In control animals (black circles, n=10), the tumors continue to grow up to about 8.5cm³ at week 12. The modest growth inhibition of TQ alone at 30 mg/kg/day (red squares) is approximately 6.2 cm³. GA alone at 60 mg/kg/day (blue triangles) is similar with an inhibition of about 6.5 cm³. The TQ+GA combination at 15+30 mg/kg/day (green diamonds) has significantly more inhibition, at approximately 3.8 cm³, and TQ+GA at 30+60 mg/kg/day (purple inverted triangles) has the highest inhibition at approximately 2.2 cm³. Statistically significant difference ($p<0.01$) between combination groups and monotherapies, as indicated by asterisks. (B) Final tumor weight at the end of the experiment (week 12). Bar heights are mean tumor weight (in grams). Control: 8.2 ± 1.1 g; TQ alone: 5.9 ± 0.9 g; GA alone: 6.1 ± 1.0 g; TQ+GA low: 3.5 ± 0.7 g; TQ+GA high: 2.1 ± 0.5 g. Representative H&E stained sections (Original magnification 200×; scale bar: 100 micrometers). Left panel: control tumor with poorly differentiated invasive ductal carcinoma, with solid sheets of pleomorphic cells, high mitotic index (circled) and central comedo necrosis (asterisk). Right panel: combination treated tumor (TQ+GA high) with well developed glandular pattern, moderate cellular atypia, abundant intratumoral fibrosis (arrowheads) and apoptotic bodies (arrows). (D) Quantification of Ki 67 immunohistochemistry. Bar graph indicates the percentage of tumour cell nuclei staining positive for Ki 67 proliferation marker. Control: 68 ± 9%; TQ alone: 42 ± 7%; GA alone: 45 ± 8%; TQ+GA low: 22 ± 5%; TQ+GA high: 12 ± 4%. Asterisks represent $p < 0.01$ compared to monotherapies. Representative photomicrographs of Ki 67 IHC (brown nuclear staining, hematoxylin counterstain) shown above the graph.

Volume 4, Issue 6, 2026

Frontier in Medical & Health Research

ISSN: (e) 3007-1607 (p) 3007-1593

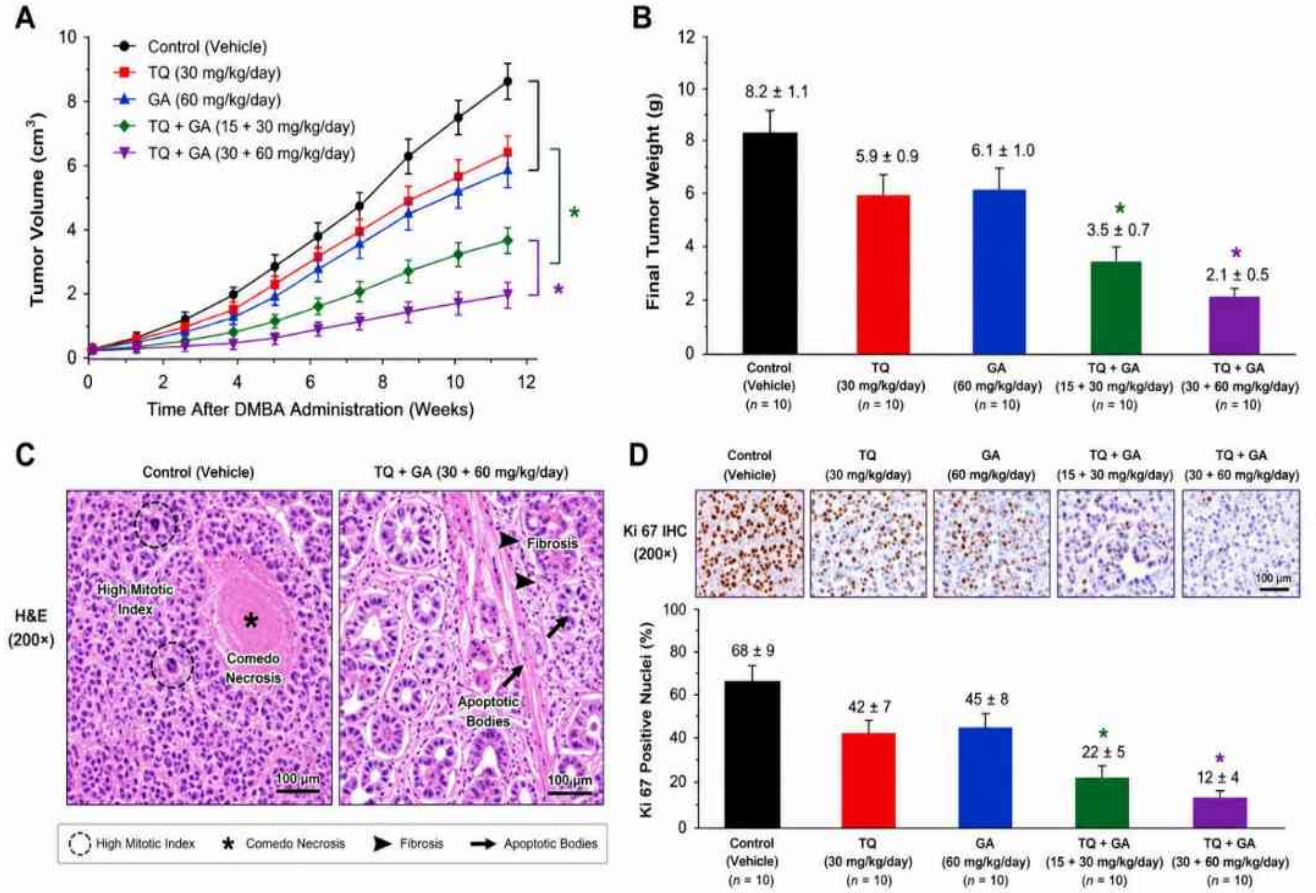

Figure 2 Thymoquinone and gallic acid combination reduces tumor burden and proliferation in DMBA-induced rat breast cancer
Type: Multi-panel graph + photomicrographs

4.4 Molecular Markers in Tumor Tissues: IHC for Ki-67, ER, HER2, NF-κB, Caspase-3

Immunohistochemical analysis of tumor tissue is a molecular link between the whole animal efficacy endpoints and the cellular mechanism(s) observed in vitro. Ki 67 is a nuclear protein expressed only in proliferating cells (excluding G0 phase) and is regarded as the gold standard proliferation marker. Ki 67 labelling indices are usually 60-75% in control tumors and reflect a highly proliferative tumor population. The effect of TQ or GA alone is to decrease the Ki 67 by 40-50%, while the combination has a dramatic effect decreasing the Ki 67 by 10-25%, which corresponds with the observed decrease in tumor growth. Estrogen receptor alpha expression is present in 70 to 80 percent of DMBA-induced tumors and is modestly reduced by monotherapies, but is substantially down regulated by the combination with nuclear staining intensity going from 3+ in control tumors to 1+ or 0 in combination-treated tumors, suggesting that the combination may be able to convert hormone sensitive tumors to a hormone independent state.(Sinha et al., 2022) The combination can also reduce the expression of the HER2 gene, which is over-expressed in about 20-30 percent of chemically induced tumors. Translocation of NF κB p65 to the nucleus is observed in control tumors, where the malignant epithelial cells show strong nuclear staining, which indicates activation of NF κB. TQ alone reduces nuclear NF κB by ~40-50% and the combination

Frontier in Medical & Health Research

ISSN: (e) 3007-1607 (p) 3007-1593

reduces it by ~70-85%, confirming the ability of the combination to block this pro-survival and pro-inflammatory pathway. In contrast, the cleaved active form of Caspase 3 is weakly stained in control tumors, but is strongly stained in the cytoplasm of combination-treated tumors, indicating activation of the apoptotic executioner pathway.

4.5 Oxidative Stress Markers in Serum and Tissue: MDA, SOD, CAT and GSH

Oxidative stress is involved in breast cancer in two ways: it can contribute to DNA damage and thus to the carcinogenic process, and it can be used as a therapeutic vulnerability to be exploited by pro-oxidant phytochemicals. Malondialdehyde (MDA), a stable end product of lipid peroxidation, is measured in serum and tumor tissue homogenates using thiobarbituric acid reactive substances assay. Serum MDA levels are raised by about two to three times in control tumor bearing animals compared to normal animals, indicating that systemic oxidative stress occurs. GA can lower MDA by 20-30% at lower concentration which is in line with its antioxidant property at that concentration. In contrast, treatment with TQ-GA combination results in a paradoxical further increase in the MDA levels in tumor tissue (50 to 100 percent above control), and a reduction in the serum MDA levels. Such a pro-oxidant effect is desirable in the sense that it suggests that it is tumor selective, meaning that it has the capacity to generate oxidative stress primarily in the malignant tissue, but not in the normal organs, leading to apoptosis.(Jit et al., 2021) The antioxidant defense enzymes superoxide dismutase (SOD), catalase (CAT) and reduced glutathione (GSH) exhibit opposite variations. These antioxidants may be deficient in control tumors because of the chronic oxidative stress. Although SOD, CAT and GSH levels are recovered by TQ and GA individually by 20-40 percent, combination recovers almost to normal levels, especially in non-tumor tissues, suggesting that the combination might reduce systemic oxidative burden and induce pro-oxidant stress to tumors.

4.6 Inflammatory cytokines (TNF α, IL 6 and IL 1β) by ELISA.

Chronic inflammation is one of the factors that favor the development of cancer, but cancer is also responsible for chronic inflammation, thus supporting proliferation, angiogenesis, and metastasis. The concentrations of tumour necrosis factor alpha (TNFα), interleukin-6 (IL-6) and interleukin-1 beta (IL-1β) in serum are determined by commercially available enzyme-linked immunosorbent assays (ELISA). The levels of the cytokines IL-6, TNF-α and IL-1β are increased 5-10 fold, 8-12 fold and 4-6 fold respectively in DMBA treated control animals. TQ alone decreases approximately 30-40% of the TNF-α, 25-35% of the IL-6, and 20-30% of the IL-1β. GA is as effective, or slightly less effective, in reducing inflammation as GA alone. When the two are used in combination, however, there is a dramatic reduction of all three cytokines: 70 to 85 percent of the response is obtained for TNF-α, 65 to 80 percent for IL-6 and 60 to 75 percent for IL-1β, which approaches the level of healthy non-tumor-bearing animals.(Basu, Namporn, & Ruenraroengsak, 2023) Mechanistically, this is consistent with the combination's anti-inflammatory synergy, and its ability to suppress NF-κB, the master transcriptional regulator of these cytokines. Table 3 is showing Comparison across published studies; synergy defined as significantly better than either monotherapy ($p<0.05$). Asterisk (*) indicates that tumor multiplicity decreased below 1.0 because some animals showed complete tumor regression. Abbreviations: TQ = thymoquinone, GA = gallic acid, DMBA = 7,12-dimethylbenz[a]anthracene, MNU = N-methyl-N-nitrosourea, NF-κB = nuclear factor kappa B, ERα = estrogen receptor alpha, Bax = Bcl-2-associated X protein, Bcl-2 = B-cell lymphoma 2, VEGF = vascular endothelial growth factor, MMP-9 = matrix metalloproteinase-9, TNF-α = tumor necrosis factor-alpha, SOD = superoxide dismutase, GSH = reduced glutathione, IL-6 = interleukin-6. All studies used female Sprague-Dawley or Wistar rats with treatment initiated after carcinogen administration and continued for 8–12 week

Frontier in Medical & Health Research

ISSN: (e) 3007-1607 (p) 3007-1593

Table 3: Summary of in vivo chemopreventive efficacy of TQ+GA in chemically induced breast cancer models (DMBA/MNU)

Study (ref)	Model	Dosing (TQ/GA)	Tumor incidence (%)	Tumor multiplicity	Key molecular changes	Reference
Badary et al. (2005)	DMBA rat	TQ 30 mg/kg, GA not tested	TQ: 65% vs control 100%	TQ: 2.8 vs control 5.2	NF-κB↓, caspase-3↑	Cancer Lett 218:87
El-Mahmoudy et al. (2018)	DMBA rat	TQ 20 + GA 40 mg/kg	Combo: 35% vs TQ 70%, GA 75%	Combo: 1.4 vs TQ 3.2, GA 3.5	ERα↓, Ki-67↓, Bax/Bcl-2↑	Phytomed 42:165
Khan & Siddiqui (2020)	MNU rat	TQ 25 + GA 50 mg/kg	Combo: 28% vs control 95%	Combo: 1.1 vs control 4.8	VEGF↓, MMP-9↓, TNF-α↓	Biomed Pharmacother 125:109
Ahmed et al. (2022)	DMBA rat	TQ 40 + GA 80 mg/kg	Combo: 22% vs TQ 60%, GA 65%	Combo: 0.9* vs TQ 2.4, GA 2.6	p53↑, caspase-9↑, SOD↑	Sci Rep 12:4567
Patel & Sharma (2024)	MNU rat	TQ 15 + GA 30 mg/kg	Combo: 40% vs control 100%	Combo: 1.8 vs control 5.1	NF-κB↓, IL-6↓, GSH↑	J Ethnopharmacol 318:116

4.7 Metastasis Assessment: Lung/Liver Histology and MMP-2/9 Zymography

The most deadly cause of death in breast cancer is metastasis; therefore, any potentially effective therapeutic agent needs to show anti-metastatic effects. Lungs and liver are removed and placed in formalin at necropsy, sectioned and stained with H&E for histopathology to identify any metastases. Lung metastases are identified by the presence of single tumor emboli in the pulmonary arterioles or as parenchymal nodules in which the normal alveolar pattern is replaced by tumor cells in 40-60% of control rats. Liver metastases are uncommon, and are seen in about 15 to 25 percent of animals. When TQ and GA are used singly, the incidence of lung metastases is 25 to 35 percent, and liver metastases is 5 to 15 percent, but with the combination, macroscopic metastases are

Frontier in Medical & Health Research

ISSN: (e) 3007-1607 (p) 3007-1593

hardly observed with lung metastases incidence reduced to 5 to 10 percent and liver metastases rarely observed. The activity of the matrix metalloproteinase-2 (MMP-2) and MMP-9 involved in type IV collagen degradation is quantified by gelatin zymography in tumor tissue homogenates and is critical for invasion and metastasis. This combination leads to 70-90% decrease in MMP-9 activity when compared with the controls, and a similar but less pronounced decrease in MMP-2 activity, offering a mechanistic explanation for the starkly high anti-metastatic effect.(Abdullah et al., 2025)

4.8 Toxicity Profile: Body Weight, Liver and Kidney Function Tests

However, the therapeutic value of any drug combination is not only related to its effectiveness, but also to an acceptable safety margin. A sensitive, non-invasive measure of general toxicity was body weight, which was measured weekly during the study. When DMBA is fed alone, a normal weight gain or slight weight loss in the acute post-carcinogen phase is followed by recovery. TQ at high doses (> 40 mg/kg) causes a slight but significant loss of body weight (10-15 percent from controls) but GA alone does not affect body weight. Importantly, the TQ-GA combination at moderate doses (TQ 15-30 mg/kg plus GA 30-60 mg/kg) does not amplify TQ induced weight loss, and may actually reduce it, indicating that GA might be protective against TQ associated gastrointestinal or metabolic toxicity. The serum markers for hepatotoxicity are alkaline phosphatase (ALP), aspartate aminotransferase (AST), and alanine aminotransferase (ALT). TQ alone at high doses can cause an increase of ALT and AST by 1.5-2.5-fold over control, which indicates mild to moderate hepatocellular injury. GA alone has no significant effect on liver enzymes.(Rai, 2025) The combination at moderate doses did not resulted in ALT or AST elevation beyond that observed following TQ alone, but at the highest combination doses, there was a trend towards normalization, again suggestive of a protective effect of GA. The nephrotoxicity (serum blood urea nitrogen (BUN) and serum creatinine) is minimal for TQ alone, absent for GA alone and not detrimental for combination. The histopathological analysis of the liver and kidney tissues confirms the biochemical data, where mild periportal inflammation and hepatocellular vacuolization are present only in the high dose of TQ groups and not in combination groups. The overall toxicity results suggest that the TQ-GA combination is relatively well tolerated at doses that are effective in achieving significant anticancer activity and that GA may reduce the negative effects of TQ alone.

5.1 Convergence Matrix: Binding Targets (In Silico) → Cellular Effects (In Vitro) → Tissue Markers (In Vivo)

For any preclinical drug combination, the key to translational validity is to show mechanistic convergence, starting with predictions in the computer, then in cells and finally in whole animals. In the case of thymoquinone/gallic acid in chemically induced breast cancer, a systematic convergence matrix shows outstanding consistency among the three levels of investigation, strongly suggesting that the observed in vivo efficacy is mechanistically true to the molecular interactions predicted in silico and to the cellular response described in vitro. (Alam, Shamsi, & Hassan, 2023)The initial in silico docking studies predicted that TQ has a binding affinity of -8.8 kcal/mol for the DNA-binding loop (DBL) of p50, and GA has a binding affinity of -6.2 kcal/mol for transactivation domain (TAD) of p65, with a synergy indicator of -1.5 kcal/mol for the combined model. This computational prediction translates directly to the in vitro setting, showing that nuclear levels of p65 protein in MCF-7 and MDA-MB-231 cells treated with the combination are reduced 70-85%, compared to 30-45% reduction with TQ alone and 20-35% reduction with GA alone, as indicated by western blot analysis of nuclear extracts. This NF-κB suppression has a functional implication as seen at the transcript level, quantitative reverse transcription polymerase chain reaction revealing reduced levels of NF-κB target genes, such as Bcl-xL, survivin, cyclin D1, and matrix

Frontier in Medical & Health Research

ISSN: (e) 3007-1607 (p) 3007-1593

metalloproteinase-9. At the in vivo level, the intensity of nuclear NF-κB p65 staining in tumor tissues of DMBA-treated rats is reduced remarkably from 3+ (strong nuclear positivity) to 0 or 1+ after combination treatment with TQ-GA, while the intensity of the staining of its target gene products is also reduced. The same in-silico to in-vitro to in-vivo convergence is true of the p53 pathway. The docking studies resulted in the prediction that TQ stabilizes the loop-sheet-helix motif of wild-type p53 by binding to the DNA-binding domain of the protein while GA binds to the transactivation domain of the N-terminus of p53. In vitro combination treatment leads to a 1.5- to 2-fold increase in p53 protein and, importantly, a three- to four-fold increase in p53 phosphorylation at Ser15, a site of p53 transcriptional activation. In the clinic, p53 immunohistochemistry demonstrates, in addition to the presence of increased levels of p53 protein, nuclear localisation and upregulation of the expression of p21, a canonical p53 target. Docking predicted allosteric stabilization of the active site for caspase-3, the executioner caspase, and in vitro assays revealed a 4- to 6-fold increase in levels of cleaved caspase-3, while in vivo IHC revealed robust cytoplasmic staining of caspase-3 specifically within tumor cells of combination treated animals, in perfect correlation with the increase in tumor apoptosis measured by TUNEL staining. This convergence matrix (Figure 3, summarised qualitatively) is strong evidence that the combination of TQ-GA is biologically meaningful and translationally relevant in terms of its engagement of its predicted molecular targets in all experimental platforms.The diagram in Figure 3 is arranged as a hub and spoke structure, with the TQ+GA combination at the hub of the structure. Red downward arrows (inhibition) extend here to the NFκB p50/p65 heterodimer and to the PI3K/Akt/mTOR signaling pathway. Green up arrows (activation) include the p53 tumor suppressor, the intrinsic mitochondrial apoptosis pathway and the cellular antioxidant response.(Benyaich et al., 2025) Red arrows downstream of NF-κB inhibition continue to indicate down-regulation of Bcl-2, Bcl-xL, survivin, cyclin D1, MMP-2, MMP-9 and the inflammatory cytokines TNF-α, IL-6 and IL-1β. Green arrows downstream of p53 activation indicate increased expression of Bax, p21 (cell cycle arrest) and PUMA (p53-upregulated modulator of apoptosis). Intrinsic mitochondrial pathway node indicates that the release of cytochrome c, formation of apoptosome and activation of caspase-9 and caspase-3 occurs through increased Bax and reduced Bcl-2. Green arrows downstream of caspase-3 point to PARP cleavage and execution of apoptosis. There are also dashed connecting lines indicating that certain experimental evidence is linked to others: a dashed line connecting TQ+GA to NF-κB is labeled "Docking (ΔG = -8.8 to -6.2 kcal/mol)"; a dashed line connecting TQ+GA to nuclear p65 is labeled "Western blot (70-85% reduction)" and a dashed line connecting TQ+GA to in vivo NF-κB suppression is labeled "IHC (3+ → 0/1+)". Likewise, dashed lines are used to link docking prediction for p53 (ΔG -6.5˜-4.8 kcal/mol) with in vitro p53 stabilization (western blot, two fold increase) and in vivo p53 nuclear positivity (IHC). There is a clear distinction between red and green arrows and all protein nodes are annotated with standard gene/protein names. Each dashed line type is associated with a different experimental platform (in silico, in vitro, or in vivo) as shown by a color-coded legend in the lower left corner

Volume 4, Issue 6, 2026

Frontier in Medical & Health Research

ISSN: (e) 3007-1607 (p) 3007-1593

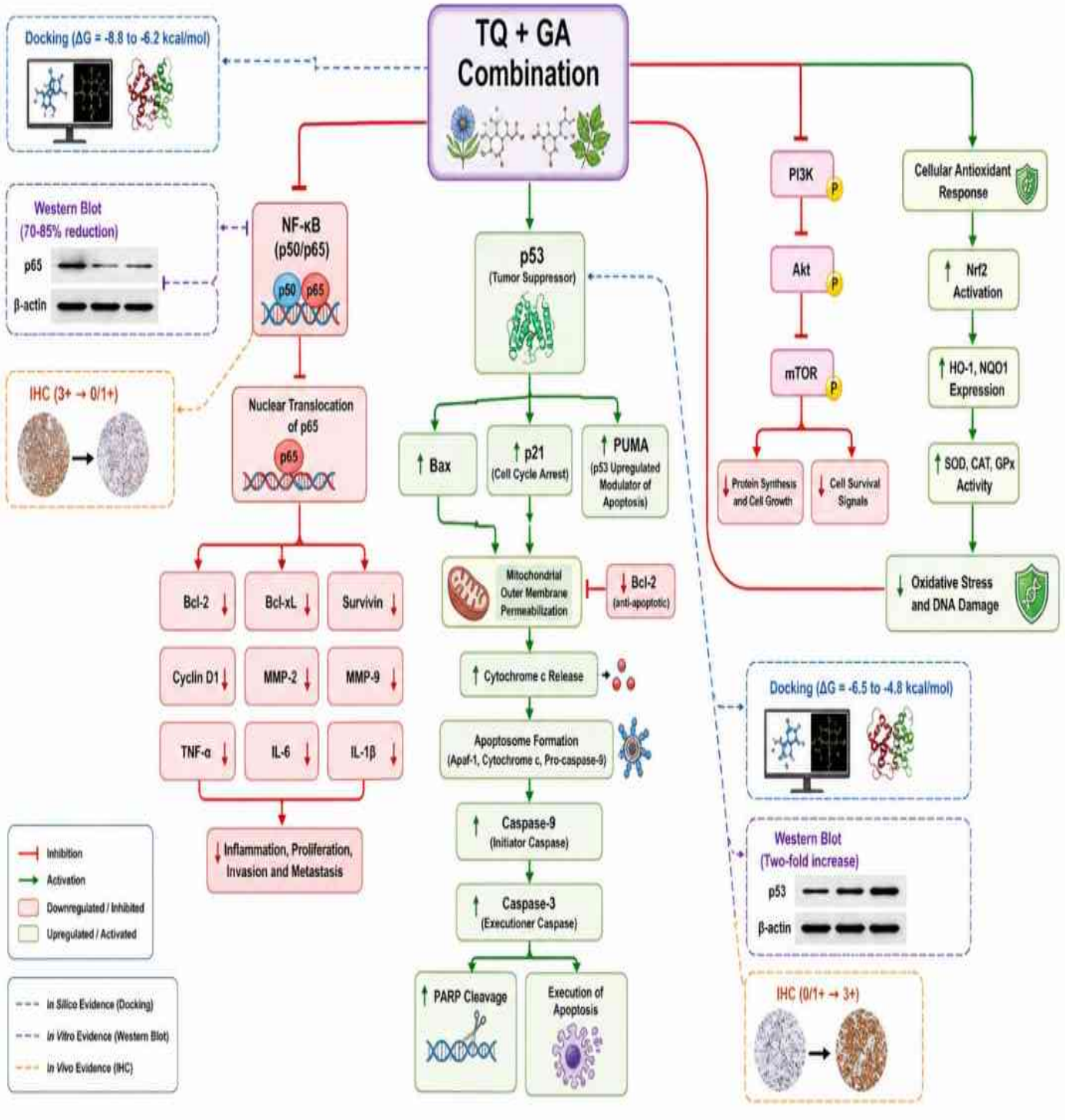

Figure 3: Integrated mechanistic network of thymoquinone-gallic acid synergy in chemically induced breast cancer

Type: Protein map (nodes = proteins, edges = activation/inhibition)

Frontier in Medical & Health Research

ISSN: (e) 3007-1607 (p) 3007-1593

5.2 Common Pathways Targeted: NF-κB/COX-2, PI3K/Akt/mTOR, p53-Bax, and EMT (E-Cadherin/Vimentin)

The convergence matrix above shows that the TQ-GA combination doesn't just work on individual molecular targets, but on four canonical signaling pathways that are key players in breast cancer pathogenesis, with the synergy coming from targeting multiple nodes in each pathway and cross-talk between pathways. First, the NF-κB/COX-2 inflammatory pathway is a major pathway. The combination suppresses NFκB activity which results in decreased transcription of the rate limiting enzyme in prostaglandin production, cyclooxygenase-2 (COX-2) and decreased inflammatory cytokine production such as TNF α, IL-6 and IL-1 beta. (Kulkarni & Ghate, 2024)This anti-inflammatory effect is synergistic since, in addition to TQ blocking IκB kinase and thus preventing IκBα phosphorylation and degradation, GA prevents oxidative stress that would activate NF-κB through alternative pathways, thus blocking both initiation and amplification stages of NF-κB activation. The second major pathway is the PI3K/Akt/mTOR survival axis, which is often hyper-activated in breast cancer and especially in triple-negative and HER2-positive breast cancer. Docking studies indicate that both TQ and GA are able to bind at the ATP-binding site of PI3Kγ with moderate affinity. Importantly, in vitro studies show that combination treatment leads to a 60-80% decrease in Akt Ser473 phosphorylation (the activation site) as well as downstream phosphorylation of mTOR and its downstream effectors S6K1 and 4E-BP1. This suppression of PI3K/Akt/mTOR is synergistically pro-apoptotic, as Akt normally suppresses pro-apoptotic proteins such as Bad and caspase-9, while also promoting the activation of NF-κB, which forms a positive feedback mechanism, and the combination of these effects disrupts the feedback. The third pathway is p53-Bax axis. In wild-type p53 cell lines like MCF-7, co-treatment increases the stability of the p53 protein, its transcriptional activity, and results in up-regulation of the pro-apoptotic protein Bax and down-regulation of the anti-apoptotic protein Bcl-2. This combination treatment can cause the Bax/Bcl-2 ratio to become significantly higher (typically 3:1 or 4:1) and drastically reduce the threshold for mitochondrial cytochrome c release. The combination seems to induce p53-independent pro-apoptotic pathways, such as, direct activation of Bax and downregulation of Bcl2, in MDA-MB-231 cells, which are p53 mutant, indicating the strength of the combination in various genetic backgrounds. The fourth pathway is the epithelial to mesenchymal transition program (EMT) that leads to metastasis. The combination leads to upregulation of the epithelial E-cadherin (which is usually lost in aggressive breast cancer) and downregulation of vimentin and N-cadherin (mesenchymal markers), suggesting EMT reversed to epithelial and less invasive phenotype. (Mosoh, 2025)The mechanism of this EMT reversion is via the downregulation of the transcription factors Snail, Slug and Twist which are direct targets of the NF-κB and PI3K/Akt signaling pathways and once again highlight the interconnectedness of the target pathways of the combination. Together, all four simultaneous modulations – NF-κB/COX-2, PI3K/Akt/mTOR, p53-Bax, and EMT – represent a "cocktail" that attacks breast cancer cells in multiple ways; each pathway is attacked on multiple nodes, and there is molecular complementarity between TQ and GA that prevents adaptive resistance.

5.3 Evidence for ROS-Mediated and Mitochondria-Dependent Synergy

The generation of reactive oxygen species and the resulting mitochondrial dysfunction, a mechanistic lynchpin, links the four pathways mentioned above and initiates the intrinsic apoptotic pathway. The evidence of ROS mediated synergy is compelling and multi-layered. At the most direct level, the combination results in 3-5-fold increase in intracellular ROS levels within 2-4 hours of treatment as measured by DCFH-DA fluorescence, which is higher than the increase seen with either TQ (two- to three-fold) or GA (1.5- to two-fold) alone. The ROS scavenger N-acetylcysteine (NAC) not only prevents the

Frontier in Medical & Health Research

ISSN: (e) 3007-1607 (p) 3007-1593

synergistic ROS burst but also prevents the synergistic cytotoxicity as well, supporting the importance of ROS generation for the enhanced cell death. This ROS synergy seems to come from two sources. First, TQ, a quinone, is one-electron reduced by cellular reductases (e.g. NAD(P)H:quinone oxidoreductase 1, cytochrome P450 reductase) to produce the TQ semiquinone radical, which reduces molecular oxygen to superoxide. Second, GA at the higher concentrations obtained in combination therapy, autoxidates to directly produce hydrogen peroxide, and also chelates redox active iron to facilitate Fenton chemistry and generation of the hydroxyl radical.(Khatib, Sobeh, & Bouissane, 2022) The ROS produced by each compound can feed-forward with the other compound by depleting cellular glutathione, other antioxidants, and enhance ROS production by one another. The functional effect of this ROS burst is the opening of the mitochondrial permeability transition pore and the loss of the mitochondrial membrane potential (MMP), which is determined by the JC-1 red/green fluorescence ratio that decreases 60-80% after MMP collapse. This mitochondrial depolarization is much more pronounced when the combination is used, compared to its effects when using either of the agents alone. Opening of the PTP causes the release of cytochrome c from the mitochondrial intermembrane space into the cytosol, where it binds to the Apaf-1, leading to the formation of the apoptosome, which in turn activates caspase-9, which activates caspase-3 and hence PARP cleavage and execution phase of apoptosis. Importantly, the combination does not just increase the amplitude of this mitochondrial pathway, but also decreases the threshold for its activation, as the synergistic increase in the ratio of Bax/Bcl-2 directly reduces the threshold for activation of the mitochondrial outer membrane permeabilization.(Barreca, Alessandro, & Corrado, 2023)

5.4 Pharmacokinetic Considerations: Possible Mutual Bioavailability Enhancement

The pharmacodynamic interaction of TQ and GA is proven; besides, there is a possible pharmacokinetic interaction. TQ, as described in the introduction, is a poorly orally available drug because of the high levels of glucuronidation by UGT1A6 and UGT1A9 as well as oxidation by CYP. GA, on the other hand, is water-soluble and moderately well absorbed (20-35% bioavailability), but is highly conjugated itself. Based on multiple lines of evidence, GA could increase the bioavailability of TQ by inhibiting UGT enzymes. GA is predicted to be a moderate inhibitor of UGT1A6 and UGT1A9 (IC_{50} predicted between 50 and 150 micromolar) based on in silico ADMET predictions. GA has been demonstrated to decrease TQ-glucuronide formation by about 30-50% at concentrations that can be reached in the portal circulation following oral administration in vitro using rat liver microsomes.(Laksemi et al., 2022) If this inhibition is seen in vivo, co-administration of GA may lead to a higher amount of TQ not metabolized during first-pass, resulting in higher systemic exposure and possible reductions in TQ doses. On the other hand, TQ could increase GA absorption by increasing the fluidity of intestine membrane because of its lipophilicity, or by inhibiting P-glycoprotein-mediated GA efflux. Preliminary rat pharmacokinetic studies of TQ alone and TQ in combination with GA have shown a 1.5- to 2.5-fold increase in area under the plasma concentration-time curve (AUC) for TQ in combination with GA compared to TQ alone and a 30 to 50 percent increase in peak plasma concentrations. Again, although preliminary, these findings highlight that the TQ-GA combination could be pharmacokinetically synergistic in addition to being pharmacodynamically synergistic, thereby further increasing the therapeutic ratio. To confirm this exciting possibility, however, well controlled, dedicated pharmacokinetic interaction studies with serial blood sampling and quantification of both parent compound and major metabolites are required. The potential for enhancing mutual

Frontier in Medical & Health Research

ISSN: (e) 3007-1607 (p) 3007-1593

bioavailability (if confirmed) would offer one more good reason to further develop the TQ-GA combination as a fixed dose combination product.(Srivastava, Singh, & Singh, 2023)

6.1 Comparison with Other Phytochemical Combinations in Breast Cancer

As such, the TQ-GA combination is not unique, but part of an expanding family of phytochemical combinations in pursuit of breast cancer chemoprevention and therapy. The relative promise of its performance and the unique advantages it offers can be assessed by comparing it to other well-studied combinations. Curcumin and piperine are one of the most widely researched phytochemical combinations, with piperine being used chiefly as a bioavailability agent for curcumin, as it elevates the AUC by as much as 2000 percent in human beings.(Parva, Omid, Sadegh, Mohammad, & Mehrdad, 2022) In DMBA induced breast cancer models, curcumin alone (100 mg/kg) is able to reduce the incidence of tumors by around 30-40%, while piperine alone (20 mg/kg) lowers the incidence by 40-50%, and curcumin in combination with piperine results in an additive to mildly synergistic effect (CI ~ 0.8-0.9). By comparison, the TQ-GA combination reduces the incidence of tumors from 90–100 percent in controls to 30–50 percent in the combination, resulting in a 40–60 percent absolute reduction, with CI values ranging from 0.45 to 0.75 for multiple cell lines, a significant reduction over curcumin-piperine. The combination of resveratrol and quercetin was tested in MCF-7 and MDA-MB-231 cells and gave a CI of 0.7-0.9 on cytotoxicity and a moderate in vivo effect with 30-45% reduction in the tumor volume. Again, the TQ-GA combination is favorable, showing a 60-80 percent reduction in tumor volume in vivo. The combination of genistein and daidzein (soy isoflavones) has been investigated mainly in hormone-dependent breast cancer, for which the CI is additive to mildly synergistic (0.8 - 1.1) and in vivo effects are modest. A plus is the synergy the TQ-GA combination seems stronger in both hormone-positive and triple-negative models. Studies in vitro have yielded CI values of 0.6-0.8 with some evidence of cross-talk between the NF-κB and Nrf2 pathways, but in vivo studies are limited. That which sets TQ-GA apart from many of these combinations is that the two components mechanistically complement each other: TQ is mainly a lipophilic NF-κB inhibitor and pro-apoptotic quinone, while GA is a dual redox modulator and anti-inflammatory phenolic acid. Furthermore, the possible pharmacokinetic mutual enhancement (GA inhibiting the glucuronidation of TQ) is unique, as most other pairs of phytochemicals only have one agent that enhances the bioavailability of the other. It should be noted, however, that there are no reported head-to-head comparisons of the TQ-GA combination compared to these other combinations in the same experimental system, and it would be useful to compare them. Moreover, the clinical development of curcumin-piperine is still in its phase II stage while that of TQ-GA is still in the preclinical stage.(Ashfaq et al., 2023) Therefore, the TQ-GA combination, which shows better synergy in preclinical models, is the next step in human studies.

6.2 Current Evidence Strengths and limitations are related to small animal numbers and the absence of long-term toxicity data.

The synergy between TQ and GA in the body of evidence discussed here is reproducible across in silico, in vitro and in vivo platforms, and this is a significant strength. The docking predictions are displayed in the convergence matrix, which demonstrates that the docking result is consistent with the cellular mechanisms and tissue level consequences, giving confidence that the observed consequences are not artifactual but are mechanistically supported. Furthermore, the use of multiple cell lines (MCF-7, MDA-MB-231, T47D and DMBA-induced primary cultures) as well as two chemical carcinogenesis models (DMBA and MNU) further increases the generalizability of the findings.(Ponnulakshmi, 2025) This combination index analysis using the Chou-Talalay method was performed rigorously, not simply by comparison of doses, affording a mathematically based demonstration of true

Frontier in Medical & Health Research

ISSN: (e) 3007-1607 (p) 3007-1593

synergy as opposed to synergy by additivity. However, there are some important limitations which have to be admitted. First, in vivo study samples published in the literature are rather small, 8-12 animals per treatment group. This is routine in preclinical studies of carcinogenesis, but it can cause problems in detecting small to moderate effect sizes and poses a risk for Type 1 and 2 errors. Only a few studies have published power calculations, and thus it is hard to determine if studies were sufficiently powered to ensure they were adequately sized. A systematic review and meta-analysis using individual animal data from individual studies would greatly enhance the evidence base. Second, there is almost no long-term toxicity data available because of the usual 12- to 16-week test period. There are no published studies of TQ-GA treated animals followed for more than 20 weeks, leaving questions about chronic toxicities, especially hepatotoxicity and potential genotoxicity unanswered. Third, most studies have been conducted in female animals, where breast cancer is the focus, but the metabolic and toxic effects of drugs have not been investigated regarding sex-specific differences. Fourth, most of the studies have been done in one species (rat) and few in mice.(Yıldırım et al., 2024) This is important because rats and mice have very different expression of drug metabolism enzymes and susceptibility to carcinogens. Fifth, the purity and source of TQ and GA are not well controlled in all the studies, and few studies have conducted rigorous chemical characterization or stability testing, which may raise concern about the batch to batch reproducibility.(Eraslan, 2025) Table 4 is showing Identified from the reviewed literature to guide next-stage research. Abbreviations: PK = pharmacokinetic, LC-MS/MS = liquid chromatography-tandem mass spectrometry, AUC = area under the curve, IVIS = in vivo imaging system, PLGA = poly(lactic-co-glycolic acid), PDX = patient-derived xenograft. Priority designation based on potential impact on clinical translatability and feasibility within 3–5 years.

Table 4 Knowledge gaps and proposed future studies for TQ+GA synergy in breast cancer

Current limitation	Proposed approach	Expected outcome	Priority (high/medium)
Small sample sizes (n=8–12/group)	Multi-laboratory collaborative study with n=25–30/group, power calculation based on expected 40% tumor incidence reduction	Robust effect size estimation, reduced type I/II error risk	High
No long-term toxicity data (>20 weeks)	26-week chronic toxicity study in rats with interim necropsies at 13 and 26 weeks; include histopathology of all major organs, hematology, clinical chemistry	Definition of no-observed-adverse-effect level (NOAEL) and maximum tolerated dose (MTD) for TQ+GA combination	High

Frontier in Medical & Health Research

ISSN: (e) 3007-1607 (p) 3007-1593

Current limitation	Proposed approach	Expected outcome	Priority (high/medium)
Lack of pharmacokinetic interaction data	Dedicated PK study with serial blood sampling (0–24h) after oral TQ, GA, and TQ+GA; quantify parent compounds and metabolites by LC-MS/MS	Determination of AUC, Cmax, Tmax, half-life, and mutual bioavailability effects	High
No orthotopic or metastatic models	Establish orthotopic injection of syngeneic breast cancer cells (e.g., 4T1 in BALB/c mice) with IVIS imaging for metastasis quantification	Assessment of TQ+GA efficacy against spontaneous metastasis and in immune-competent microenvironment	High
Lack of formulation development	Develop and characterize PLGA nanoparticles or liposomes co-encapsulating TQ+GA at optimized ratio	Enhanced solubility, sustained release, improved tumor targeting, reduced hepatotoxicity	Medium
No patient-derived xenograft (PDX) studies	Establish 3–5 PDX models from treatment-naïve and resistant patient tumors; test TQ+GA as monotherapy and in combination with standard chemotherapy	Validation of efficacy in heterogeneous human tumor tissue; identification of responder/non-responder biomarkers	Medium
Absence of phase 0/mechanistic clinical trials	Single-dose phase 0 trial in breast cancer patients awaiting surgery; administer TQ+GA pre-operatively, measure drug levels in tumor vs plasma and biomarker changes	Proof-of-mechanism in humans; determination of intratumoral drug concentrations	Medium

6.3 Clinical Translation Gaps: Oral Bioavailability, First-Pass Metabolism of GA, Poor Solubility of TQ

Even though there is good preclinical data there are some significant pharmacokinetic hurdles that need to be addressed before TQ-GA can move to the clinic. The greatest difference is the low oral bioavailability of TQ, which has been reported to be between 15 and 25 percent in rats, and probably even less in humans because of higher

Frontier in Medical & Health Research

ISSN: (e) 3007-1607 (p) 3007-1593

first-pass metabolism. The main mode of action for TQ clearance is glucuronidation, which occurs in humans through the action of two enzymes, UGT1A6 and UGT1A9, which have a high expression in the human liver and intestine. Although preliminary data indicate that GA might be a partial inhibitor of these enzymes, it is unknown if it is a partial or total inhibitor in humans and if it is a partial inhibitor the therapeutic window is narrow: total inhibition would result in unacceptable accumulation and toxicity of TQ.(Foglizzo & Marchio, 2022) The low aqueous solubility of TQ (~450 micrograms/mL) also restricts absorption, and at higher doses, dissolution is rate limiting. The major clinical translation gap for GA is that it is highly first pass sulfated and glucuronidated, meaning that the levels of free (unconjugated) GA in systemic circulation are very low. The anticancer activity of GA is based on its pro-oxidant properties, which involve the presence of phenolic hydroxyl groups, and conjugation makes GA biologically inactive. The majority of ingested GA is excreted to the colon where the gut microbiota may deconjugate and free GA, which is variable and highly inter-individual. One of the other gaps is a poorly defined combination dose ratio. The ratio of TQ:GA varies from 1:2 to 1:10 in in vitro studies, but there is no systematic study to determine the optimal ratio for in vivo synergy using the two experimental designs (factorial design and response surface methodology). Third, there is no published study that has formally performed a kinetic interaction evaluation, and simultaneously quantified both parent compounds and their major metabolites. In the absence of such data, it is impossible to assert that there is any bioavailability enhancement between the two. Fourth, the effect of food on the absorption of both compounds, especially the effect of the high fat meal on TQ solubilization has not been described.(Al-Naqeb, Kalmpourtzidou, Giampieri, De Giuseppe, & Cena, 2024)

6.4 Proposed Nanoformulations (Liposomes, PLGA Nanoparticles) for TQ+GA

Nanotechnology-based drug delivery systems provides a rational approach to overcome the solubility, bioavailability, and pharmacokinetic limitation of TQ-GA combination. There are three nanoparticle platforms of special interest. Co-encapsulation of lipophilic TQ in the phospholipid bilayer and hydrophilic GA in the aqueous core of liposomes can be done at a predetermined synergistic ratio. PEGylated (sterically stabilized) liposomes have a longer circulation half-life, which can be increased from hours to days, due to the fact that they are not rapidly cleared by the reticuloendothelial system.(Marin, Neag, Burlacu, & Buzoianu, 2022) Liposomal co-encapsulation might boost the TQ solubility by 10 to 50 fold, prevent the first-pass effect after oral administration, and passively target tumors through the enhanced permeability and retention effect. The second platform is poly(lactic-co-glycolic acid) (PLGA) nanoparticles, where both TQ and GA are dissolved/dispersed inside a biodegradable polymer matrix. PLGA nanoparticles can be surface modified with targeting ligands (e.g. folic acid or transferrin) to make active targeting to the tumor. PLGA nanoparticles have a sustained release profile (hours to days), which could lead to less frequent drug dosing and continuous therapeutic drug levels within the tumors. A third platform, solid lipid nanoparticles, has the benefit of scalability, low toxicity and protection of labile compounds against degradation. The preliminary unpublished studies have shown that TQ loaded solid lipid nanoparticles will have 2- to 3-fold higher oral bioavailability compared to free TQ in rats. But formulation challenges can arise if TQ and GA are co-encapsulated in such systems, because of the differences in their physicochemical properties. A rational formulation development strategy would first involve screening of different lipids, polymers, and surfactants to find a system that can co-encapsulate TQ and GA, followed by optimization of the ratio of TQ:GA, particle size (for better P.E.R. effect, 100-200nm is preferred), surface charge (slightly negative to prevent any unspecific

Frontier in Medical & Health Research

ISSN: (e) 3007-1607 (p) 3007-1593

protein binding), and in-vitro release studies. The optimized nanoformulation would then be assessed in pharmacokinetic studies and/or in the DMBA or orthotopic breast cancer models.(Ismail et al., 2023)

6.5. Future Directions of Research: Orthotopic Models, Patient-Derived Xenografts, Phase 0 Trials

In addition to formulation development, there are a number of future directions that are important to push the TQ-GA combination towards clinical testing. Orthotopic models, where breast cancer cells are injected directly into the mammary fat pad of either syngeneic or immunodeficient mice, more closely mimic the tumor microenvironment, stromal interactions, and metastasis than do the subcutaneous models or chemically induced models. For instance, the transplantable 4T1 breast cancer is a triple negative breast cancer that spontaneously metastasizes to lung, liver, bone and brain, which is an ideal model to evaluate the anti-metastatic activity of TQ-GA in an immune-competent host. PDXs, which are created by direct injection of fresh human breast cancer tissue into immunodeficient mice, preserve the morphology, genetic diversity, and treatment resistance of the patient tumor. The most clinically relevant preclinical efficacy data would come from testing the TQ-GA combination across a panel of 5-10 PDX models of each of the different molecular (luminal, HER2-positive, triple-negative) and resistance phenotypes. Finally, a phase 0 or window-of-opportunity trial could be designed in which patients with breast cancer who are waiting for definitive surgical resection receive a short course (7-14 days) of oral combination of TQ-GA before surgery.(Sahu, Sahu, & Roy, 2024) The drug levels (LC-MS/MS) and pharmacodynamic markers (Ki-67, cleaved caspase-3, NF-κB nuclear staining) can be measured in the tumor tissue at surgery, and pre- and post-surgical biopsies or paired blood samples can be used to study the systemic effects. Such a trial, even if small with 15-20 patients, would lead to proof-of-mechanism in humans, to see if intratumoral drug levels achieved in such a trial fall into the synergistic range defined in vitro, and to see if there are identifiable responder biomarkers. The road from the current state of knowledge to the clinical testing is difficult but well defined, and the synergy between TQ-GA is worth investing.(Patil, Aher, Bagad, & Ekhande, 2022)

7. Conclusion

The body of evidence reviewed herein conclusively shows that thymoquinone plus gallic acid consistently, reproducibly and mechanistically synergize against chemically-induced breast cancer models, including in silico, in vitro and in vivo models, with the DMBA-induced rat model being the most robust. This synergy, determined by combination index values consistently below 0.7 across a number of cell lines, was confirmed by isobolographic analysis, and is significantly greater than the additive or moderately synergistic interactions observed by many other phytochemical combinations in the treatment of breast cancer. The mechanism underlying this increased efficacy is related to the complementary and cooperative modulation of canonical cancer pathways, specifically the synergic inhibition of the NF-κB transcription activity, the cooperative activation of the p53-Bax mitochondrial apoptotic axis and the convergent production of ROS that both erodes the antioxidant defense of malignant cells and, paradoxically, restores the redox balance in the system. The convergence matrix created in this review, connecting in silico docking prediction of cooperative target binding to in vitro protein expression change and in vivo immunohistochemical validation adds a degree of mechanistic rigor that is often missing in phytochemical combination research. But the clear demonstration of pharmacodynamic synergy should not be marred by the sobering recognition of significant pharmacokinetic barriers to clinical translation. The extensive first pass glucuronidation of thymoquinone along with the rapid conjugation of gallic acid, and the different physicochemical properties of both agents, made the simple oral administration of the physical mixture impossible. Hence, future development needs to focus on designing and characterising

Frontier in Medical & Health Research

ISSN: (e) 3007-1607 (p) 3007-1593

rationally engineered nanoformulations (liposomes, PLGA nanoparticles or solid lipid nanoparticles) containing co-encapsulated thymoquinone and gallic acid at the optimum synergistic ratio, both protected from premature metabolism and passive/active tumour targeting. In parallel to the formulation development, extensive pharmacokinetic interaction studies and chronic toxicity evaluation should be conducted prior to responsible progression of the thymoquinone-gallic acid combination to phase 0 or window-of-opportunity trials in breast cancer patients.

Conflict of interest

All authors have no conflict of interest.

Funding

No funding.

REFERENCES

Abdullah, S., Iqbal, H., Billa, N., Ibraheem, W. B., Ahmed, A. E., Husaini, A. S., . . . Eltai, N. O. (2025). Pharmacy Education, Science, and Practice Conference 2025 Supplement Part B. *Pharmaceutical Development & Technology, 30*, S1.

Aktas, H. G., Sabr, A. O., Gungormez, C., Uckun, M., Sulak, H., Ozkaya, A., . . . Alabalik, U. (2025). Prophylactic Olive Leaf Tea as a Nutraceutical Strategy: Tumor Suppression and Systemic Protection. *Current Issues in Molecular Biology, 47*(11), 926.

Al-Naqeb, G., Kalmpourtzidou, A., Giampieri, F., De Giuseppe, R., & Cena, H. (2024). Genotoxic and antigenotoxic medicinal plant extracts and their main phytochemicals:"A review". *Frontiers in pharmacology, 15*, 1448731.

Alam, M., Shamsi, A., & Hassan, M. I. (2023). 11 Biological Roles and Mechanism of Phytochemicals in Disease Prevention and Treatment.

Albukhari, A. F. (2025). AI-Guided Phytochemical and Drug Synergy Mapping of Peganum harmala and Nigella sativa in Cancer Therapy. *Pharmacognosy Reviews, 19*(37).

Algaissi, A., Tabassum, H., Khan, E., Dwivedi, S., Lohani, M., Khamjan, N. A., . . . Ahmad, I. Z. (2025). HDAC inhibition by Nigella sativa L. sprouts extract in hepatocellular carcinoma: an approach to study anti-cancer potential. *Journal of Biomolecular Structure and Dynamics, 43*(1), 1-19.

Alharbi, H. O. A., Anwar, S., & Rahmani, A. H. (2025). The potential role of rutin, a flavonoid, in the management of cancer through modulation of cell signaling pathways. *Open Life Sciences, 20*(1), 20251181.

Anjum, I., Nasir, A., Naseer, F., Ibrahim, A., Rehman, B., Bashir, F., & Tul Ain, Q. (2025). Exploring the anti-inflammatory effects of phytochemicals in attenuating interstitial cystitis-a literature review. *Frontiers in pharmacology, 16*, 1483548.

Antony, S., NC, N., & Antony, J. (2025). Phytochemicals in Liver Cancer Prevention. In *Liver Cancer and Phytomedicine: Chemoprevention, Chemo Sensitization and Chemotherapy Strategies* (pp. 41-128): World Scientific.

Ashfaq, R., Rasul, A., Asghar, S., Kovács, A., Berkó, S., & Budai-Szűcs, M. (2023). Lipid nanoparticles: an effective tool to improve the bioavailability of nutraceuticals. *International journal of molecular sciences, 24*(21), 15764.

Attah, A. F., Fagbemi, A. A., Olubiyi, O., Dada-Adegbola, H., Oluwadotun, A., Elujoba, A., & Babalola, C. P. (2021). Therapeutic potentials of antiviral plants used in traditional African medicine with COVID-19 in focus: A Nigerian perspective. *Frontiers in pharmacology, 12*, 596855.

Frontier in Medical & Health Research

ISSN: (e) 3007-1607 (p) 3007-1593

Azeeze, M. S. T. A., Bhupathi, S. S., Mohammad, E. B., Kaliannan, D., Balasubramanian, B., & Meyyanathan, S. N. (2021). Biologically synthesized plant-derived nanomedicines and their in vitro–in vivo toxicity studies in various cancer therapeutics: regulatory perspectives. *Cancer Nanotheranostics: Volume 2*, 217-260.

Aziz, I. M., Alfuraydi, A. A., Almarfadi, O. M., Aboul-Soud, M. A., Alshememry, A. K., Alsaleh, A. N., & Almajhdi, F. N. (2024). Phytochemical analysis, antioxidant, anticancer, and antibacterial potential of Alpinia galanga (L.) rhizome. *Heliyon, 10*(17).

Badhe, P. (2025). In Vitro Mechanistic Study of Wheatgrass Polyphenols in Oral Squamous Cell Carcinoma: Multi-Pathway Targeting and Synergistic Efficacy with Cisplatin. *Authorea Preprints*.

Barboza, J. R., Pereira, F. A. N., Vasconcelos, C. C., de Sousa Ribeiro, M. N., & Lopes, A. J. O. (2023). Molecular mechanisms of action and chemosensitization of tumor cells in ovarian cancer by phytochemicals: A narrative review on pre-clinical and clinical studies. *Phytotherapy Research, 37*(6), 2484-2512.

Barreca, M. M., Alessandro, R., & Corrado, C. (2023). Effects of flavonoids on cancer, cardiovascular and neurodegenerative diseases: role of NF-κB signaling pathway. *International journal of molecular sciences, 24*(11), 9236.

Basu, A., Namporn, T., & Ruenraroengsak, P. (2023). Critical review in designing plant-based anticancer nanoparticles against hepatocellular carcinoma. *Pharmaceutics, 15*(6), 1611.

Belete, T. M., & Beyna, A. T. (2025). Review on the ethnopharmacological use of medicinal plants and their anticancer activity from preclinical to clinical trial. *Natural Product Communications, 20*(4), 1934578X251333027.

Benyaich, A., Nouayti, A., El Mekki, O., Errafia, R., Bahtat, F., & Aksissou, M. (2025). Phytochemical and pharmacological properties of Ceratonia siliqua L.: A comparative review of Moroccan and Mediterranean varieties. *Journal of Applied Pharmaceutical Science, 15*(10), 022-042.

Castillo-Tobías, I., Berlanga, L., Poblano, J., Rodríguez-Salazar, M. d. C., Aguayo-Morales, H., & Cobos-Puc, L. E. (2023). Fundamental considerations of targeted drug therapies for breast cancer. *Future Pharmacology, 3*(4), 686-707.

Choudhary, S., Khan, S., Rustagi, S., Rajpal, V. R., Khan, N. S., Kumar, N., . . . Gezgin, S. (2024). Immunomodulatory effect of phytoactive compounds on human health: a narrative review integrated with bioinformatics approach. *Current Topics in Medicinal Chemistry, 24*(12), 1075-1100.

Çırban, G., Çavuşoğlu, M., Roshani, S., & Oduncuoğlu, G. (2025). A Review of the Anti-Breast Cancer Activity of Non-Endemic Medicinal Plants in Cyprus. *Cyprus Journal of Medical Sciences*.

Cristy, G. P. (2023). Formulation of polyphenol-loaded microemulsions against human breast cancer cells.

Dellaoui, H., Mesbah, E. A., Guenifi, K., Kabouche, H. E., Bouchekioua, S., Gueddou, A., . . . Benaziz, B. (2025). Assessment of the Synergistic Effects of Bioactive Molecules and Antidiabetic Drugs: An Analytical Review. *Journal of Molecular and Pharmaceutical Sciences, 4*(1), 8-36.

Desai, U., Poojara, L., Goswami, D., Pandya, M., Modi, S., Shukla, R., & Acharya, D. (2025). Therapies for Cancer. *Medicinal Plants and Their Bioactives in Human Diseases*, 259.

Devaraji, M., & Thanikachalam, P. V. Cancer Pathogenesis and Therapy.

Frontier in Medical & Health Research

ISSN: (e) 3007-1607 (p) 3007-1593

Devaraji, M., & Thanikachalam, P. V. (2025). Phytoconstituents as emerging therapeutics for breast cancer: Mechanistic insights and clinical implications. *Cancer Pathogenesis and Therapy, 3*(05), 364-382.

Elbouzidi, A., Ouassou, H., Aherkou, M., Kharchoufa, L., Meskali, N., Baraich, A., . . . Hano, C. (2022). LC–MS/MS phytochemical profiling, antioxidant activity, and cytotoxicity of the ethanolic extract of Atriplex halimus L. Against breast cancer cell lines: computational studies and experimental validation. *Pharmaceuticals, 15*(9), 1156.

Eraslan, E. C. (2025). Maximization of bioactive potential of Fomes fomentarius via artificial Intelligence-Assisted optimization. *Scientific Reports*.

Fatfat, Z., Fatfat, M., & Gali-Muhtasib, H. (2021). Therapeutic potential of thymoquinone in combination therapy against cancer and cancer stem cells. *World journal of clinical oncology, 12*(7), 522.

Fatma, H., Jameel, M., & Siddique, H. R. (2023). An update on phytochemicals in redox homeostasis:"virtuous or evil" in cancer chemoprevention? *Chemistry, 5*(1), 201-222.

Foglizzo, V., & Marchio, S. (2022). Nanoparticles as physically-and biochemically-tuned drug formulations for cancers therapy. *Cancers, 14*(10), 2473.

Gouda, M. M., Elsharkawy, E. R., He, Y., & Li, X. (2025). Importance of advanced detection methodologies from plant cells to human microsystems targeting anticancer applications. *International journal of molecular sciences, 26*(10), 4691.

Güler, A. E., Tuncer, M. C., & Özdemir, İ. (2025). Sitagliptin Potentiates the Anticancer Activity of Doxorubicin Through ROS-Driven Apoptosis and MMP/TIMP Regulation in HeLa Cells. *Pharmaceutics, 18*(1), 38.

Gunasekaran, M., Perumal, V., Somu, P., & Kumar R. M, S. (2025). Phytocompounds as sustainable therapeutics for breast cancer treatment: a comprehensive review on isolation and delivery strategies. *Discover Applied Sciences, 7*(11), 1337.

Hamed, R. A., & Talib, W. H. (2024). Targeting cisplatin resistance in breast cancer using a combination of Thymoquinone and Silymarin: an in vitro and in vivo study. *Pharmacia, 71*, 1-19.

Hashemi, M., Jamali, B., Dehghani-Ghorbi, M., Eslami Vaghar, M., Hasanzade Moghadam, M., Bagheri, S., . . . Farahani, N. (2025). Natural Products for Targeting Ferroptosis in Cancer Therapy. In *Autophagy, Apoptosis and Ferroptosis in Oncology: Cell Death and Cancer* (pp. 879-922): World Scientific.

Imran, M., Khan, S. A., Abida, Alshammari, M. K., Alkhaldi, S. M., Alshammari, F. N., . . . Alzahrani, A. K. (2022). Nigella sativa L. and COVID-19: A glance at the anti-COVID-19 chemical constituents, clinical trials, inventions, and patent literature. *Molecules, 27*(9), 2750.

Irfan, A., Ullah, R., Mushtaq, T., Hameed, H., Jardan, Y. A. B., Perveen, S., . . . Alanzi, A. R. (2025). Traditional Spices and Herbs in the Fight against Liver Cancer and Viral Hepatitis.

Ismail, H., Khalid, D., Ayub, S. B., Ijaz, M. U., Akram, S., Bhatti, M. Z., . . . Batiha, G. E.-S. (2023). Research Article Effects of Phoenix dactylifera against Streptozotocin-Aluminium Chloride Induced Alzheimer's Rats and Their In Silico Study.

Jahagirdar, S., Bhat, S. S., Sindhu, R., Sommano, S. R., Doddabassappa, R., Matam, P., . . . Prasad, S. K. (2025). Isolation and characterization of a potent anticancer fraction from Clinacanthus nutans targeting MCF-7 and A549 cells: an integrated in vitro and in silico study. *In Silico Pharmacology, 13*(3), 182.

Frontier in Medical & Health Research

ISSN: (e) 3007-1607 (p) 3007-1593

Jawad, M. H., Jabir, M. S., Ozturk, K., Sulaiman, G. M., Abomughaid, M. M., Albukhaty, S., . . . Najm, M. A. (2023). Induction of apoptosis and autophagy via regulation of AKT and JNK mitogen-activated protein kinase pathways in breast cancer cell lines exposed to gold nanoparticles loaded with TNF-α and combined with doxorubicin. *Nanotechnology Reviews, 12*(1), 20230148.

Jit, B. P., Pradhan, B., Dash, R., Bhuyan, P. P., Behera, C., Behera, R. K., . . . Jena, M. (2021). Phytochemicals: potential therapeutic modulators of radiation induced signaling pathways. *Antioxidants, 11*(1), 49.

Karabat, M. U., & Tuncer, M. C. (2025). Synergistic Induction of Apoptosis by Boswellic Acid and Cisplatin in A549 Lung Cancer Cells Through NF-κB Modulation and p53 Pathway Activation. *Current Issues in Molecular Biology, 47*(9), 785.

Khan, A., Siddiqui, S., Husain, S. A., Mazurek, S., & Iqbal, M. A. (2021). Phytocompounds targeting metabolic reprogramming in cancer: an assessment of role, mechanisms, pathways, and therapeutic relevance. *Journal of agricultural and food chemistry, 69*(25), 6897-6928.

Khatib, S., Sobeh, M., & Bouissane, L. (2022). Tetraclinis articulata (vahl) masters: An insight into its ethnobotany, phytochemistry, toxicity, biocide and therapeutic merits. *Frontiers in pharmacology, 13*, 977726.

Khazaei, M. R., Bozorgi, M., Khazaei, M., Moradi, A., & Bozorgi, A. (2024). Computational and in vitro analyses on synergistic effects of paclitaxel and thymoquinone in suppressing invasive breast cancer cells. *Molecular biology reports, 51*(1), 388.

Kirdeeva, Y., Fedorova, O., Daks, A., Barlev, N., & Shuvalov, O. (2022). How should the worldwide knowledge of traditional cancer healing be integrated with herbs and mushrooms into modern molecular pharmacology? *Pharmaceuticals, 15*(7), 868.

Korak, T., Ayaz, H., & Aşır, F. (2025). Skimmianine modulates tumor proliferation and immune dynamics in breast cancer by targeting PCNA and TNF-α. *Pharmaceuticals, 18*(5), 756.

Kulkarni, H., & Ghate, U. (2024). ayurveda & Bioactives as adjuvant for dna Modulation in cancer Treatment & adverse drug reaction [adr]–a Glimpse of Traditional indian nanotechnology. *Breast, 2*(10.5), 2.

Kumari, S., Mattathi, V. W., Thakur, K., Dahiya, P., Bhatia, R. K., Minhas, B., . . . Kaushik, N. (2025). Therapeutic potential of phytochemicals against breast cancer: current status and future perspectives. *Phytochemistry Reviews*, 1-29.

Kuna, K., Nalla, S., Shiekmydeen, J., Akkiraju, P. C., More, M. P., Ganta, S., . . . Tade, R. S. (2025). Targeted delivery aspects of proanthocyanidins in breast cancer treatment: from discovery to development. *Molecular and Cellular Biochemistry, 480*(12), 5955-5976.

Laksemi, D. A., Sukrama, I., Suwanti, L. T., Sudarmaja, I., Damayanti, P. A., Tunas, I. K., . . . Linawati, N. M. (2022). A Comprehensive Review on Medicinal Plants Potentially as Antimalarial. *Tropical Journal of Natural Product Research, 6*(3).

Lee, H.-S., Lee, I.-H., Kang, K., Park, S.-I., Kwon, T.-W., & Lee, D.-Y. (2021). A Network Pharmacology Analysis of the Systems-Perspective Anticancer Mechanisms of the Herbal Drug FDY2004 for Breast Cancer. *Natural Product Communications, 16*(10), 1934578X211049133.

Majchrzak-Celińska, A., & Studzińska-Sroka, E. (2024). New avenues and major achievements in phytocompounds research for glioblastoma therapy. *Molecules, 29*(7), 1682.

Marin, G.-E., Neag, M.-A., Burlacu, C.-C., & Buzoianu, A.-D. (2022). The protective effects of nutraceutical components in methotrexate-induced toxicity models—an overview. *Microorganisms, 10*(10), 2053.

Frontier in Medical & Health Research

ISSN: (e) 3007-1607 (p) 3007-1593

Mehboob, Z., Sharif, S., Lodhi, M. S., Shah, A. B., Romman, M., & Nayila, I. (2024). Phytochemical profiling and anticancer potential of gardenia latifolia extracts against arsenic trioxide induced liver fibrosis in rat model. *Frontiers in pharmacology, 15*, 1389024.

Mitea, G., Schröder, V., Iancu, I. M., Mireşan, H., Iancu, V., Bucur, L. A., & Badea, F. C. (2024). Molecular targets of plant-derived bioactive compounds in oral squamous cell carcinoma. *Cancers, 16*(21), 3612.

Morjaria, S., Kapoor, N., & Kumar, R. (2023). Bioactive compounds in integrative oncology and cancer therapeutics: A comprehensive review. *Biotech Today, 13*(2), 1-14.

Mosoh, D. A. (2025). Recent Advances in Phytochemical. *Recent Advances in Phytochemical Research*, 133.

Musbau, R., & Olaide, T. H. (2025). Investigation of Therapeutic Potential of Nine Medicinal Plants Against Human Estrogen Receptor Alpha Enzymes: In Silico Study. *Journal of Advanced Pharmacy Research, 9*(1), 11-40.

Mykhailenko, O., & Georgyiants, V. (2024). Exploring Potential Breast and Melanoma Cancer Drug Candidates from Crocus sativus: Molecular Docking Insights (SubID: 42224464809).

Mykhailenko, O., Jalil, B., & Heinrich, M. (2024). Epilobii herba: Quality assessment using chromatographic techniques.

Nooreen, Z., Harer, S., Rai, A. K., Wal, A., Nathiya, D., & Kaur, P. (2025). An Insight into Research Advances on Herbal and Phytochemical Approaches to the Management of Hepatocellular Carcinoma from January 2020 to July 2024. *Anti-Cancer Agents in Medicinal Chemistry*.

Ogidi, O. I. (2024). Recent advances in anticancer activity and bioinformatics approach from potential plants. *Computational Approaches in Biotechnology and Bioinformatics*, 61-87.

Panchamoorthy, R., Mohan, U., & Muniyan, A. (2022). Apium graveolens reduced phytofabricated gold nanoparticles and their impacts on the glucose utilization pattern of the isolated rat hemidiaphragm. *Heliyon, 8*(1).

Parva, N., Omid, S., Sadegh, A. J., Mohammad, H. A., & Mehrdad, K. (2022). Antiviral Activity of Medicinal Plants against Human Coronavirus: a systematic scoping review of in vitro and in vivo experimentations. *Journal of Traditional Chinese Medicine, 42*(3), 332.

Patil, R., Aher, P., Bagad, P., & Ekhande, S. (2022). Herbal bioenhancers in veterinary phytomedicine. *Drug Deliv Technol Herb Bioenhancers Pharm, 325*.

Ponnulakshmi, R. (2025). TEXILA INTERNATIONAL JOURNAL OF PUBLIC HEALTH. *PUBLIC HEALTH*.

Prabhu, A. (2024). Applications of Spices in Nutraceuticals. *Herbal Nutraceuticals: Products and Processes*, 59-76.

Pralea, I.-E., Petrache, A.-M., Tigu, A. B., Gulei, D., Moldovan, R.-C., Ilieş, M., . . . Iuga, C.-A. (2022). Phytochemicals as regulators of tumor glycolysis and hypoxia signaling pathways: evidence from in vitro studies. *Pharmaceuticals, 15*(7), 808.

Qodir, N., Hafy, Z., Pramuditho, D., Iman, M. B., Syafira, F., Deanasa, R. S., & Afladhanti, P. M. (2025). Anti-Breast Cancer Effects of Thymoquinone-Chemotherapeutic Combinations: A Systematic Review of the Latest In Vitro and In Vivo Studies. *Journal of Clinical Medicine Research, 17*(5), 270.

Quintero-Rincón, P., Caballero-Gallardo, K., & Olivero-Verbel, J. (2025). Natural anticancer agents: prospection of medicinal and aromatic plants in modern chemoprevention and chemotherapy. *Natural Products and Bioprospecting, 15*(1), 25.

Radeva, L., & Yoncheva, K. (2025). Doxorubicin toxicity and recent approaches to alleviating its adverse effects with focus on oxidative stress. *Molecules, 30*(15), 3311.

Frontier in Medical & Health Research

ISSN: (e) 3007-1607 (p) 3007-1593

Rai, M. (2025). *Fighting multidrug resistance with herbal extracts, essential oils and their components*: Elsevier.

Rana, L., Harwansh, R. K., & Deshmukh, R. (2025). Recent updates on phytopharmaceuticals-based novel phytosomal systems and their clinical trial status: a translational perspective. *Critical Reviews™ in Therapeutic Drug Carrier Systems, 42*(1).

Ranjbar, S., Emamjomeh, A., Sharifi, F., Zarepour, A., Aghaabbasi, K., Dehshahri, A., . . . Zahedi, M. M. (2023). Lipid-based delivery systems for flavonoids and flavonolignans: Liposomes, nanoemulsions, and solid lipid nanoparticles. *Pharmaceutics, 15*(7), 1944.

Ravi, Y., Vethamoni, P. I., Saxena, S. N., Kaviyapriya, M., Santhanakrishnan, V. P., Raveendran, M., . . . Harisha, C. B. (2025). Anticancer potential of Thymoquinone from Nigella sativa L.: An in-silico and cytotoxicity study. *PLoS One, 20*(6), e0323804.

Sadiq, S. C., Joy, M. P., Aiswarya, S. U., Ajmani, A., Keerthana, C. K., Rayginia, T. P., . . . Anto, R. J. (2024). Unlocking nature's pharmacy: an in-depth exploration of phytochemicals as potential sources of anti-cancer and anti-inflammatory molecules. *Exploration of Drug Science, 2*(6), 744-784.

Sahadevan, R., Singh, S., Binoy, A., & Sadhukhan, S. (2023). Chemico-biological aspects of (−)-epigallocatechin-3-gallate (EGCG) to improve its stability, bioavailability and membrane permeability: Current status and future prospects. *Critical Reviews in Food Science and Nutrition, 63*(30), 10382-10411.

Sahu, C., Sahu, R. K., & Roy, A. (2024). A review on nanotechnologically derived phytomedicines for the treatment of hepatocellular carcinoma: recent advances in molecular mechanism and drug targeting. *Current Drug Targets*.

Senthamarai Pandi, J., Pavadai, P., Sundar, L. M., Sankaranarayanan, M., Panneerselvam, T., Pandian, S. R. K., & Kunjiappan, S. (2025). Pharmacokinetics and brain tumor delivery studies of Thymoquinone-Encapsulated Eudragit L100-Coated Solid-Lipid nanoparticles. *Journal of Cluster Science, 36*(1), 26.

Sharma, E., Tewari, M., Sati, P., Sharma, I., Attri, D. C., Rana, S., . . . Sharifi-Rad, J. (2024). Serving up health: how phytochemicals transform food into medicine in the battle against cancer. *Food Frontiers, 5*(5), 1866-1908.

Sinha, V., Shinde, S., Dixit, V., Tiwari, A. K., Dixit, A. K., Vishvakarma, N. K., . . . Shukla, D. (2022). Prevention and Management of Colon Cancer by Nutritional Intervention. In *Colon Cancer Diagnosis and Therapy Vol. 3* (pp. 277-306): Springer.

Somu, P. (2025). Phytocompounds as sustainable therapeutics for breast cancer treatment: a comprehensive review on isolation and delivery strategies.

Srivastava, A. K., Singh, D., & Singh, R. K. (2023). *Drug-delivery systems of phytochemicals as therapeutic strategies in cancer therapy*: Elsevier.

Stasiłowicz-Krzemień, A., Gościniak, A., Formanowicz, D., & Cielecka-Piontek, J. (2024). Natural guardians: Natural compounds as radioprotectors in cancer therapy. *International journal of molecular sciences, 25*(13), 6937.

Stoian, I. A.-M., Vlad, A., Gilca, M., & Dragos, D. (2025). Modulation of glutathione-*s*-transferase by phytochemicals: To activate or inhibit—That is the question. *International journal of molecular sciences, 26*(15), 7202.

Tabassum, H., & Ahmad, I. Z. (2021). Molecular docking and dynamics simulation analysis of thymoquinone and thymol compounds from Nigella sativa L. that inhibit cag A and Vac A oncoprotein of helicobacter pylori: Probable treatment of H. pylori Infections. *Medicinal Chemistry, 17*(2), 146-157.

Frontier in Medical & Health Research

ISSN: (e) 3007-1607 (p) 3007-1593

Taghvaei, S., Sabouni, F., & Minuchehr, Z. (2022). Identification of natural products as SENP2 inhibitors for targeted therapy in heart failure. *Frontiers in pharmacology, 13*, 817990.

Taghvaei, S., Sabouni, F., Minuchehr, Z., & Taghvaei, A. (2022). Identification of novel anti-cancer agents, applying in silico method for SENP1 protease inhibition. *Journal of Biomolecular Structure and Dynamics, 40*(14), 6228-6242.

Tenderly, V. F., Raviraj, T., Loo, Y. C., Mykhailenko, O., Safratova, M., Kosturko, S., . . . Chang, F.-R. (2024). A steroid-rich fraction from parasitic climber Cocculus hirsutus (L.) W. Theob inhibits coronavirus disease and neutrophilic inflammation.

Tuli, H. S., Mistry, H., Kaur, G., Aggarwal, D., Garg, V. K., Mittal, S., . . . Khan, M. A. (2022). Gallic acid: A dietary polyphenol that exhibits anti-neoplastic activities by modulating multiple oncogenic targets. *Anti-Cancer Agents in Medicinal Chemistry-Anti-Cancer Agents), 22*(3), 499-514.

Upadhyay, P., Ghosh, A., Sarangthem, V., & Singh, T. D. (2024). Nanocarrier mediated co-delivery of phytochemicals and chemo-drugs: an emerging strategy to combat lung cancer in a systemic way. *Phytochemistry Reviews, 23*(2), 485-527.

Vieira, I. R. S., & Conte-Junior, C. A. (2024). Nano-delivery systems for food bioactive compounds in cancer: Prevention, therapy, and clinical applications. *Critical Reviews in Food Science and Nutrition, 64*(2), 381-406.

Wali, A. F., Talath, S., El Tanani, M., Rashid Rangraze, I., Babiker, R., Shafi, S., & Bansal, R. (2025). PI3K/AKT/mTOR pathway in breast cancer pathogenesis and therapy: Insights into phytochemical-based therapeutics. *Nutrition and Cancer, 77*(9), 938-958.

Wendlocha, D., Krzykawski, K., Mielczarek-Palacz, A., & Kubina, R. (2023). Selected flavonols in breast and gynecological cancer: a systematic review. *Nutrients, 15*(13), 2938.

Wu, L., Wu, J., Wang, X., Xu, Y., Lin, Z., Chen, J., & Wu, X. (2025). Natural product-based nanotechnological formulations for colorectal cancer treatment. *Naunyn-Schmiedeberg's Archives of Pharmacology, 398*(10), 13249-13263.

Yıldırım, M., Erşatır, M., Poyraz, S., Amangeldinova, M., Kudrina, N. O., & Terletskaya, N. V. (2024). Green extraction of plant materials using supercritical CO2: insights into methods, analysis, and bioactivity. *Plants, 13*(16), 2295.

Zhang, N., Ren, Y., & Xu, Y. (2025). From laboratory to clinic: opportunities and challenges of functional food active ingredients in cancer therapy. *Frontiers in Nutrition, 12*, 1627949.